Graphical Abstract

An asymptotic derivation of a single particle model with electrolyte

Scott G. Marquis, Valentin Sulzer, Robert Timms,
Colin P. Please, S. Jon Chapman

Highlights

An asymptotic derivation of a single particle model with electrolyte

Scott G. Marquis, Valentin Sulzer, Robert Timms,
Colin P. Please, S. Jon Chapman

- An extension of the single particle model which is shown to be more accurate than similar models in the literature through both mathematical argument and direct numerical comparison.
- Systematic asymptotic derivation of single particle model and electrolyte extension.
- Quantification of error of reduced model in terms of model parameters

An asymptotic derivation of a single particle model with electrolyte

Scott G. Marquis[a], Valentin Sulzer[a], Robert Timms[a,b],
Colin P. Please[a,b], S. Jon Chapman[a,b]

[a] *Mathematical Institute, University of Oxford, OX2 6GG, United Kingdom*
[b] *The Faraday Institution*

Abstract

The standard continuum model of a lithium-ion battery, the Doyle-Fuller-Newman (DFN) model, is computationally expensive to solve. Typically simpler models, such as the single particle model (SPM), are used to provide insight for control purposes. Recently, there has been a move to extend the SPM to include electrolyte effects, which increase the accuracy and range of applicability. However, these extended models are derived in an ad-hoc manner, which leaves open the possibility that important terms may have been neglected, resulting in the model not being as accurate as possible. In this paper, we provide a systematic asymptotic derivation of both the SPM and a correction term that accounts for the behaviour in the electrolyte. Firstly, this allows us to quantify the error in the reduced model in terms of ratios of key parameters in the model, from which the range of applicable operating conditions can be determined. Secondly, in comparing our model with the ad-hoc models from the literature, we show that previous models have neglected a key set of terms. In particular, we make the crucial distinction between writing the terminal voltage in pointwise and electrode-averaged form, which allows us to gain additional accuracy whilst maintaining the same computational complexity as the existing models.

Keywords: Lithium-ion batteries, Asymptotic methods, Reduced order models, Single particle model

1. Introduction

1.1. Background

Lithium-ion batteries are used extensively in consumer electronics and industry. Mathematical models are an essential tool for the design and management of battery systems. The standard mathematical model of a lithium-ion battery is the Doyle-Fuller Newman (DFN) model, which was developed by John Newman and collaborators [1, 2, 3]. This model is sometimes referred to as the pseudo two-dimensional (P2D) model or simply the Newman model. The model consists of a set of highly coupled nonlinear parabolic and elliptic partial differential equations (PDEs). This system of equations has been solved using a variety of different numerical methods: finite difference methods, control volumes, finite elements, orthogonal collocation, and others [1, 4, 5, 6, 7, 8, 9]. However, even when employing sophisticated

Email address: marquis@maths.ox.ac.uk (Scott G. Marquis)

numerical techniques, the DFN remains a computationally expensive model. For many applications, particularly within control, this level of computational complexity is not practical and so simpler models, such as the single particle model (SPM) are used [10, 11, 12, 13]. There have been several previous papers that provide justification for the SPM and suggest correction terms that may increase the accuracy of the voltage prediction it gives [14, 15, 16, 17, 18, 19]. However, these approaches generally rely on a number of ad-hoc assumptions. In this work, we provide a systematic mathematical derivation of the SPM and an additional correction for the electrolyte by applying asymptotic methods to the DFN. Asymptotic methods are widely applied within many subdisciplines of mathematics but are still relatively underutilised in battery modelling [20, 21]. They have however been successfully applied in the derivation of the DFN model (asymptotic homogenisation) and in the derivation of reduced-order lead acid battery models [22, 23]. They have also been applied to the reduction of lithium-ion battery models which neglect the effects of the particles [24] but not yet to the full DFN model. In our approach we consider approximations that can be found by exploiting two physically relevant limiting cases: first that the electrical conductivity is large in the electrodes and electrolyte, and second that the lithium ion migration timescale in the electrolyte is small relative to the typical timescale for a discharge. The validity of applying both of these limits is determined directly from the input parameter values which allows for the errors in the reduced models to be estimated a priori. By comparison, in [10] for example, six assumptions that can only be validated by comparison with the full DFN model are required (e.g. that the current profile assumes a specific form). A key result of this work is the derivation of a single additional partial differential equation and algebraic correction to the terminal voltage which accounts for nonuniform effects in the electrolyte and greatly improves the accuracy of the predictions when compared to the SPM. Additionally, we identify a key step overlooked in the ad-hoc derivations, and show through direct numerical comparison that performing this step allows our reduced model to outperform the other ad-hoc models in the literature whist retaining the same level of computational complexity.

We begin by providing a brief overview of the DFN model, after which we nondimensionalise it. At this stage, we re-write the terminal voltage in electrode-averaged form, which is essential in the derivation of our reduced models. We then identify two important physical limits: large electrical conductivity in the electrodes and electrolyte, and a small lithium ion migration timescale relative to the typical discharge timescale. We perform a systematic asymptotic reduction in the distinguished limit in which the electrical conductivities are of a comparable size to the inverse of the ratio of the lithium ion migration timescale to the typical discharge timescale. We make a uniform asymptotic expansion and, at leading order, recover the SPM. By extending the asymptotic expansion to the first order, we develop an additional PDE for the concentration of lithium-ions in the electrolyte alongside an additional algebraic correction to the terminal voltage. We summarise our reduced model and compare results with the DFN, and also with the ad-hoc models from the literature, showing that our reduced model best recovers the predictions of the DFN.

2. Doyle-Fuller-Newman (DFN) model

Lithium-ion batteries consist of two electrodes, a porous separator, an electrolyte, and two current collectors, as displayed in Figure 1. Each electrode consists of active material particles within which lithium can be stored, and a binder which holds the electrode together and maintains electrical conductivity between the active material particles. In Figure 1, we do not display the binder material.

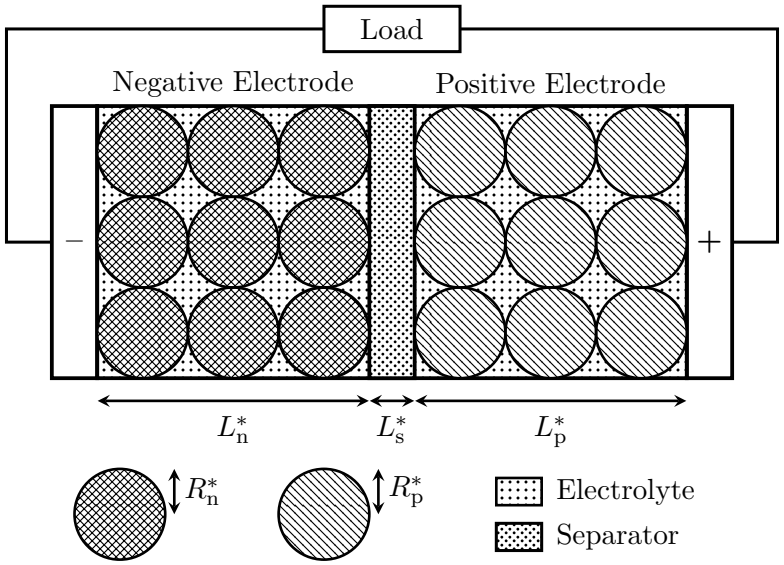

Figure 1: Schematic of a lithium-ion battery. Active material particles are shaded cross-stitch and diagonally for the negative and positive active materials, respectively.

Upon discharge, lithium intercalated in the negative electrode particles diffuses to the surface of the particles where an electrochemical reaction occurs. This electrochemical reaction produces a lithium ion free to move through the electrolyte and an electron free to move through the electrode. The electron travels through the electrode, into the current collector, through an external wire, and towards the positive electrode. Meanwhile, the lithium ion migrates through the electrolyte towards the positive electrode. At the surface of the positive electrode particles, the lithium ion and the electron combine through another electrochemical reaction to form a lithium atom intercalated in the positive electrode particle. To charge the battery, a voltage is applied across the cell and the whole process occurs in reverse.

We summarise here the DFN model which is the standard model of a lithium-ion battery [1, 2, 3]. The model is derived either by volume averaging [3] or the method of multiple scales [22]. Throughout, we use a superscript $*$ to indicate dimensional quantities. As indicated in Figure 1, the thickness's of the negative electrode, separator, and positive electrode are L_{n}^*, L_{s}^*, and L_{p}^*, respectively. We denote the distance between the negative and positive current collectors by $L^* = L_{\mathrm{n}}^* + L_{\mathrm{s}}^* + L_{\mathrm{p}}^*$. The active material particles in the negative and positive electrodes are assumed to be spheres with radii R_{n}^* and R_{p}^*, respectively. Additionally, we assume that the behaviour within the particles is spherically symmetric. We use the spatial coordinate $x^* \in [0, L^*]$ to indicate the location through the thickness of the battery and the spatial coordinate $r^* \in [0, R_{\mathrm{k}}^*]$, $\mathrm{k} \in \{\mathrm{n}, \mathrm{p}\}$ to indicate the location within the particles of

active material. We define the following regions of the battery,

$$\Omega_{\mathrm{n}}^* = [0, L_{\mathrm{n}}^*], \quad \Omega_{\mathrm{s}}^* = [L_{\mathrm{n}}^*, L^* - L_{\mathrm{p}}^*], \quad \Omega_{\mathrm{p}}^* = [L^* - L_{\mathrm{p}}^*, L^*],$$

which correspond to the negative electrode, separator, and positive electrode regions, respectively. We denote electric potentials by ϕ^*, current densities by i^*, lithium concentrations by c^* (in the electrolyte c^* refers to lithium ion concentrations), and molar fluxes by N^*. To indicate the region within which each variable is defined, we include a subscript $\mathrm{k} \in \{\mathrm{n}, \mathrm{s}, \mathrm{p}\}$ which corresponds to Ω_{n}^*, Ω_{s}^*, and Ω_{p}^*, respectively. To distinguish variables in the electrolyte from those in the solid phase of the electrode, we employ an additional subscript e for electrolyte variables and an additional subscript s for solid phase variables. For clarity, the variables in the model and their corresponding regions are

$$\begin{aligned}
&\phi_{\mathrm{s,n}}^*,\ \phi_{\mathrm{e,n}}^*,\ c_{\mathrm{e,n}}^*,\ i_{\mathrm{e,n}}^*,\ N_{\mathrm{e,n}}^* : && && x^* \in \Omega_{\mathrm{n}}^*,\\
&\phi_{\mathrm{e,s}}^*,\ c_{\mathrm{e,s}}^*,\ i_{\mathrm{e,s}}^*,\ N_{\mathrm{e,s}}^* : && && x^* \in \Omega_{\mathrm{s}}^*,\\
&\phi_{\mathrm{s,p}}^*,\ \phi_{\mathrm{e,p}}^*,\ c_{\mathrm{e,p}}^*,\ i_{\mathrm{e,p}}^*, N_{\mathrm{e,p}}^* : && && x^* \in \Omega_{\mathrm{p}}^*,\\
&c_{\mathrm{s,n}}^* : && r^* \in [0, R_{\mathrm{n}}^*], && x^* \in \Omega_{\mathrm{n}}^*,\\
&c_{\mathrm{s,p}}^* : && r^* \in [0, R_{\mathrm{p}}^*], && x^* \in \Omega_{\mathrm{p}}^*.
\end{aligned}$$

We note that $c_{\mathrm{s,n}}^*$ and $c_{\mathrm{s,p}}^*$ are dependent on the macroscopic spatial variable, x^*, the microscopic spatial variable, r^*, and time, t^* whereas, all other variables depend on x^* and t^* only. When stating the governing equations, we take the region in which an equation holds to be automatically defined by the subscript, $\mathrm{k} \in \{\mathrm{n}, \mathrm{s}, \mathrm{p}\}$, of the variables. With this in mind, the 1+1D DFN model is summarised as:

Governing Equations

Charge Conservation:

$$\frac{\partial i_{\mathrm{e,k}}^*}{\partial x^*} = \begin{cases} a_{\mathrm{k}}^* j_{\mathrm{k}}^*, & \mathrm{k} = \mathrm{n},\ \mathrm{p}, \\ 0, & \mathrm{k} = \mathrm{s}, \end{cases} \tag{1a}$$

$$i_{\mathrm{e,k}}^* = \epsilon_{\mathrm{k}}^b \kappa_{\mathrm{e}}^*(c_{\mathrm{e,k}}^*) \left(-\frac{\partial \phi_{\mathrm{e,k}}^*}{\partial x^*} + 2(1 - t^+) \frac{R^* T^*}{F^*} \frac{\partial}{\partial x^*} \left(\log\left(c_{\mathrm{e,k}}^*\right) \right) \right), \qquad \mathrm{k} \in \{\mathrm{n}, \mathrm{s}, \mathrm{p}\}, \tag{1b}$$

$$I^* - i_{\mathrm{e,k}}^* = -\sigma_{\mathrm{k}}^* \frac{\partial \phi_{\mathrm{s,k}}^*}{\partial x^*}, \qquad \mathrm{k} \in \{\mathrm{n}, \mathrm{p}\} \tag{1c}$$

Molar Conservation:

$$\epsilon_{\mathrm{k}} \frac{\partial c_{\mathrm{e,k}}^*}{\partial t^*} = \frac{\partial N_{\mathrm{e,k}}^*}{\partial x^*} + \frac{1}{F^*} \frac{\partial i_{\mathrm{e,k}}^*}{\partial x^*}, \qquad \mathrm{k} \in \{\mathrm{n}, \mathrm{s}, \mathrm{p}\}, \tag{1d}$$

$$N_{\mathrm{e,k}}^* = \epsilon_{\mathrm{k}}^b D_e^*(c_{\mathrm{e,k}}^*) \frac{\partial c_{\mathrm{e,k}}^*}{\partial x^*} + \frac{t^+}{F^*} i_{\mathrm{e,k}}^*, \qquad \mathrm{k} \in \{\mathrm{n}, \mathrm{s}, \mathrm{p}\}, \tag{1e}$$

$$\frac{\partial c_{\mathrm{s,k}}^*}{\partial t^*} = \frac{1}{(r^*)^2} \frac{\partial}{\partial r^*} \left((r^*)^2 D_{\mathrm{s,k}}^* \frac{\partial c_{\mathrm{s,k}}^*}{\partial r^*} \right), \qquad \mathrm{k} \in \{\mathrm{n}, \mathrm{p}\}, \tag{1f}$$

Electrochemical Reactions:

$$j_{\mathrm{k}}^* = j_{0,\mathrm{k}}^* \sinh\left(\frac{F^*\eta_{\mathrm{k}}^*}{2R^*T^*}\right), \qquad \mathrm{k} \in \{\mathrm{n},\, \mathrm{p}\}, \tag{1g}$$

$$j_{0,\mathrm{k}}^* = m_{\mathrm{k}}^*(c_{\mathrm{s,k}}^*)^{1/2}(c_{\mathrm{s,k,max}}^* - c_{\mathrm{s,k}}^*)^{1/2}(c_{\mathrm{e,k}}^*)^{1/2} \qquad \mathrm{k} \in \{\mathrm{n},\, \mathrm{p}\}, \tag{1h}$$

$$\eta_{\mathrm{k}}^* = \phi_{\mathrm{s,k}} - \phi_{\mathrm{e,k}}^* - U_{\mathrm{k}}^*(c_{\mathrm{s,k}}^*\big|_{r^*=R_{\mathrm{k}}^*}), \qquad \mathrm{k} \in \{\mathrm{n},\, \mathrm{p}\}, \tag{1i}$$

Boundary Conditions

Current in Electrolyte:

$$i_{\mathrm{e,n}}^*\big|_{x^*=0} = i_{\mathrm{e,p}}^*\big|_{x^*=L^*} = 0, \tag{1j}$$

$$\phi_{\mathrm{e,n}}^*\big|_{x^*=L_{\mathrm{n}}^*} = \phi_{\mathrm{e,s}}^*\big|_{x^*=L_{\mathrm{n}}^*}, \quad i_{\mathrm{e,n}}^*\big|_{x^*=L_{\mathrm{n}}^*} = i_{\mathrm{e,s}}^*\big|_{x^*=L_{\mathrm{n}}^*} = I^*, \tag{1k}$$

$$\phi_{\mathrm{e,s}}^*\big|_{x^*=L^*-L_{\mathrm{p}}^*} = \phi_{\mathrm{e,p}}^*\big|_{x^*=L^*-L_{\mathrm{p}}^*}, \quad i_{\mathrm{e,s}}^*\big|_{x=L^*-L_{\mathrm{p}}^*} = i_{\mathrm{e,p}}^*\big|_{x^*=L^*-L_{\mathrm{p}}^*} = I^*, \tag{1l}$$

Concentration in Electrolyte:

$$N_{\mathrm{e,n}}^*\big|_{x^*=0} = 0, \quad N_{\mathrm{e,p}}^*\big|_{x^*=L^*} = 0, \tag{1m}$$

$$c_{\mathrm{e,n}}^*|_{x^*=L_{\mathrm{n}}^*} = c_{\mathrm{e,s}}^*|_{x^*=L_{\mathrm{n}}^*}, \quad N_{\mathrm{e,n}}^*\big|_{x^*=L_{\mathrm{n}}^*} = N_{\mathrm{e,s}}^*\big|_{x^*=L_{\mathrm{n}}^*}, \tag{1n}$$

$$c_{\mathrm{e,s}}^*|_{x^*=L^*-L_{\mathrm{p}}^*} = c_{\mathrm{e,p}}^*|_{x^*=L^*-L_{\mathrm{p}}^*}, \quad N_{\mathrm{e,s}}^*\big|_{x^*=L^*-L_{\mathrm{p}}^*} = N_{\mathrm{e,p}}^*\big|_{x^*=L^*-L_{\mathrm{p}}^*}, \tag{1o}$$

Concentration in Electrode Active Material:

$$\left.\frac{\partial c_{\mathrm{s,k}}^*}{\partial r^*}\right|_{r^*=0} = 0, \quad -D_{\mathrm{s,k}}^* \left.\frac{\partial c_{\mathrm{s,k}}^*}{\partial r^*}\right|_{r^*=R_{\mathrm{k}}^*} = \frac{j_{\mathrm{k}}^*}{F^*}, \quad \mathrm{k} \in \{\mathrm{n},\, \mathrm{p}\}, \tag{1p}$$

Reference Potential

$$\phi_{\mathrm{s,n}}^*\big|_{x^*=0} = 0, \tag{1q}$$

Initial Conditions

$$c_{\mathrm{s,k}}^*(x^*, r^*, 0) = c_{\mathrm{s,k,0}}^* \qquad \mathrm{k} \in \{\mathrm{n},\, \mathrm{p}\}, \tag{1r}$$

$$c_{\mathrm{e,k}}^*(x^*, 0) = c_{\mathrm{e,typ}}^*, \qquad \mathrm{k} \in \{\mathrm{n},\, \mathrm{s},\, \mathrm{p}\}. \tag{1s}$$

The functional forms for $U_{\mathrm{n}}^*(c_{\mathrm{s,n}}^*)$, $U_{\mathrm{p}}^*(c_{\mathrm{s,p}}^*)$, and $D_{\mathrm{e}}^*(c_{\mathrm{e}}^*)$, which are the open circuit potentials (OCP) at the negative and positive electrodes and the lithium ion diffusivity in the electrolyte respectively, are taken from Newman's Dualfoil code [25]. A full list of parameters and their values is provided in Table 1. The values in this table are taken from Scott Moura's fastDFN code [26], which are in turn adapted from the parameter values used in Newman's Dualfoil code [25]. These functions and parameters correspond to a cell with a graphite negative electrode, a $LiPF_6$ in EC:DMC electrolyte, and a lithium cobalt oxide positive electrode. In (1c), (1j), and (1k) the actual current density I^* is distinct from the typical current density I_{typ}^* in Table 1. We make this distinction to easily accommodate non-constant currents within the dimensionless form of our reduced models.

Parameter	Units	Description	Ω_n^*	Ω_s^*	Ω_p^*
ϵ_{k}	-	Electrolyte volume fraction	0.3	1	0.3
$c_{k,\max}^*$	$\mathrm{mol/m^3}$	Maximum lithium concentration	2.4983×10^4	-	5.1218×10^4
σ_{k}^*	S/m	Solid conductivity	100	-	10
$D_{\mathrm{s,k}}^*$	$\mathrm{m^2/s}$	Electrode diffusivity	3.9×10^{-14}	-	1×10^{-13}
R_{k}^*	µm	Particle radius	10	-	10
a_{k}^*	$\mu\mathrm{m}^{-1}$	Electrode surface area density	0.18	-	0.15
m_{k}^*	$(\mathrm{A/m^2})(\mathrm{m^3/mol})^{1.5}$	Reaction rate	2×10^{-5}	-	6×10^{-7}
L_{k}^*	µm	Thickness	100	25	100
$U_{\mathrm{k,ref}}^*$	V	Reference open circuit potential	0.18	-	3.94
$c_{e,\mathrm{typ}}^*$	$\mathrm{mol/m^3}$	Typical lithium ion concentration in electrolyte		1×10^3	
$D_{\mathrm{e,typ}}^*$	$\mathrm{m^2/s}$	Typical electrolyte diffusivity		5.34×10^{-10}	
$\kappa_{\mathrm{e,typ}}^*$	S/m	Typical electrolyte conductivity		1.1	
F^*	C/mol	Faraday's constant		96485	
R_g^*	J/(mol K)	Universal gas constant		8.314472	
T^*	K	Temperature		298.15	
b	-	Bruggeman coefficient		1.5	
t^+	-	Transference number		0.4	
I_{typ}^*	$\mathrm{A/m^2}$	Typical current density		24 (1 C)	

Table 1: Dimensional model parameters with values taken from [26].

3. Asymptotic reduction of DFN model

3.1. Dimensionless form of DFN model

We use asymptotic methods to systematically reduce the DFN model to simpler forms. To do this, we first nondimensionalise the DFN model by making the following scalings:

$$
\begin{aligned}
&\text{Global:} && x^* = L^* x, \quad t^* = \tau_{\mathrm{d}}^* t, \quad D_{\mathrm{e}}^* = D_{\mathrm{e,typ}}^* D_{\mathrm{e}}, \\
& && \kappa_{\mathrm{e}}^* = \kappa_{\mathrm{e,typ}}^* \kappa_{\mathrm{e}} \quad I^* = I_{\mathrm{typ}}^* I \\
& && \phi_{\mathrm{s,n}}^* = \frac{R^* T^*}{F^*} \phi_{\mathrm{s,n}}, \quad \phi_{\mathrm{s,p}}^* = \left(U_{\mathrm{p,ref}}^* - U_{\mathrm{n,ref}}^*\right) + \frac{R^* T^*}{F^*} \phi_{\mathrm{p,k}}, \\
&\text{For k} \in \{\text{n, p}\}: && r_{\mathrm{k}}^* = R_{\mathrm{k}}^* r_{\mathrm{k}}, \quad c_{\mathrm{s,k}}^* = c_{\mathrm{s,k,max}}^* c_{\mathrm{s,k}}, \\
& && j_{\mathrm{k}}^* = \frac{I_{\mathrm{typ}}^*}{a_{\mathrm{k}}^* L^*} j_{\mathrm{k}}, \quad j_{0,\mathrm{k}}^* = \frac{I_{\mathrm{typ}}^*}{a_{\mathrm{k}}^* L^*} j_{0,\mathrm{k}}, \quad m_{\mathrm{k}}^* = m_{\mathrm{k,typ}}^* m_{\mathrm{k}}, \\
& && \eta_{\mathrm{k}}^* = \Phi^* \eta_{\mathrm{k}}, \quad U_{\mathrm{k}}^* = U_{\mathrm{k,ref}}^* + \frac{R^* T^*}{F^*} U_{\mathrm{k}}, \\
&\text{For k} \in \{\text{n, p}\}: && i_{\mathrm{s,k}}^* = I_{\mathrm{typ}}^* i_{\mathrm{s,k}}, \\
&\text{For k} \in \{\text{n, s, p}\}: && c_{\mathrm{e,k}}^* = c_{\mathrm{e,typ}}^* c_{\mathrm{e,k}}, \quad N_{\mathrm{e,k}}^* = \frac{D_{\mathrm{e,typ}}^* c_{\mathrm{e,typ}}^*}{L^*} N_{\mathrm{e,k}}, \\
& && \phi_{\mathrm{e,k}}^* = -U_{\mathrm{n,ref}}^* + \frac{R^* T^*}{F^*} \phi_{\mathrm{e,k}}, \quad i_{\mathrm{e,k}}^* = I_{\mathrm{typ}}^* i_{\mathrm{e,k}}.
\end{aligned}
\tag{2}
$$

We then identify the key timescales in the model, which are presented in Table 2. We also identify a set of dimensionless parameters, which are provided in terms of the dimensional variables alongside their physical meaning and calculated values in Table 3.

Symbol	Expression	Interpretation	Value [s]
τ_{d}^*	$F^* c_{\mathrm{n,max}}^* L^* / I_{\mathrm{typ}}^*$	Discharge timescale	$2.2598 \times 10^4 / \mathcal{C}$
τ_{n}^*	$(R_{\mathrm{n}}^*)^2 / D_{\mathrm{s,p}}^*$	Diffusion timescale in the negative electrode particle	2.5641×10^3
τ_{p}^*	$(R_{\mathrm{p}}^*)^2 / D_{\mathrm{s,p}}^*$	Diffusion timescale in the positive electrode particle	1×10^3
τ_{e}^*	$(L^*)^2 / D_{\mathrm{e,typ}}^*$	Diffusion timescale in the electrolyte	94.803
$\tau_{\mathrm{r,n}}^*$	$F^* / (m_{\mathrm{n}}^* a_{\mathrm{n}}^* (c_{\mathrm{e,typ}}^*)^{1/2})$	Reaction timescale in the negative electrode	847.534
$\tau_{\mathrm{r,p}}^*$	$F^* / (m_{\mathrm{p}}^* a_{\mathrm{p}}^* (c_{\mathrm{e,typ}}^*)^{1/2})$	Reaction timescale in the positive electrode	3.3901×10^4

Table 2: Timescales associated with the physical processes occurring within the battery model; $\mathcal{C}$ is the C-rate.

Parameter	Expression	Interpretation	n	s	p
L_{k}	L_{k}^* / L^*	Ratio of region thickness to cell thickness	0.4444	0.1111	0.4444
$\mathcal{C}_{\mathrm{k}}$	$\tau_{\mathrm{k}}^* / \tau_{\mathrm{d}}^*$	Ratio of solid diffusion and discharge timescales	$0.1134\,\mathcal{C}$	-	$0.0442\,\mathcal{C}$
$\mathcal{C}_{\mathrm{r,k}}$	$\tau_{\mathrm{r,k}}^* / \tau_{\mathrm{d}}^*$	Ratio of reaction and discharge timescales	$0.0375\,\mathcal{C}$	-	$1.5\,\mathcal{C}$
σ_{k}	$(R^*T^*/F^*) / ((I_{\mathrm{typ}}^* L^* / \sigma_{\mathrm{k}}^*))$	Ratio of thermal voltage and typical ohmic drop in the solid	$475.791/\mathcal{C}$	-	$47.5791/\mathcal{C}$
a_{k}	$a_{\mathrm{k}}^* R_{\mathrm{k}}^*$	Product of particle radius and surface area density	1.8	-	1.5
γ_{k}	$c_{\mathrm{k,max}}^* / c_{\mathrm{n,max}}^*$	Ratio of maximum lithium concentrations in solid	1	-	2.0501
$\mathcal{C}_{\mathrm{e}}$	$\tau_{\mathrm{e}}^* / \tau_{\mathrm{d}}^*$	Ratio of electrolyte transport and discharge timescales		$4.19 \times 10^{-3}\,\mathcal{C}$	
γ_{e}	$c_{\mathrm{e,typ}}^* / c_{\mathrm{n,max}}^*$	Ratio of maximum lithium concentration in the negative electrode solid and typical electrolyte concentration		0.04	
$\hat{\kappa}_{\mathrm{e}}$	$(R^*T^*/F^*) \,/\, ((I_{\mathrm{typ}}^* L^* / \kappa_{\mathrm{e,typ}}^*))$	Ratio of thermal voltage to the typical ohmic drop in the electrolyte		$5.2337/\mathcal{C}$	
$c_{\mathrm{k},0}$	$c_{\mathrm{k},0}^* / c_{\mathrm{k,max}}^*$	Ratio of initial lithium concentration to maximum lithium concentration in solid	0.8	-	0.6

Table 3: Typical dimensionless parameter values. Here $\mathcal{C} = I^*/(24\,\mathrm{A\,m^{-2}})$ is the C-Rate where we have taken a 1C rate to correspond to a typical x-direction current density of $24\,\mathrm{A\,m^{-2}}$. This is for a cell with an initial stoichiometry of 0.8 in the negative electrode and 0.6 in the positive electrode with a voltage cutoff of 3.2 V.

Inserting the scalings (2) in the dimensional model (1), we obtain the dimensionless version of the model which is summarised as:

Governing equations

Charge conservation:

$$\frac{\partial i_{\mathrm{e,k}}}{\partial x} = \begin{cases} j_{\mathrm{k}}, & \mathrm{k} = \mathrm{n},\, \mathrm{p} \\ 0, & \mathrm{k} = \mathrm{s} \end{cases}, \tag{3a}$$

$$i_{\mathrm{e,k}} = \epsilon_{\mathrm{k}}^{\mathrm{b}} \hat{\kappa}_{\mathrm{e}} \kappa_{\mathrm{e}}(c_{\mathrm{e,k}}) \left(-\frac{\partial \phi_{\mathrm{e,k}}}{\partial x} + 2(1 - t^+) \frac{\partial}{\partial x} \left(\log(c_{\mathrm{e,k}}) \right) \right), \qquad \mathrm{k} \in \{\mathrm{n},\, \mathrm{s},\, \mathrm{p}\}, \tag{3b}$$

$$I - i_{\mathrm{e,k}} = -\sigma_{\mathrm{k}} \frac{\partial \phi_{\mathrm{k}}}{\partial x}, \qquad \mathrm{k} \in \{\mathrm{n},\, \mathrm{p}\}, \tag{3c}$$

Molar conservation:

$$\mathcal{C}_{\mathrm{e}}\epsilon_{\mathrm{k}}\gamma_{\mathrm{e}}\frac{\partial c_{\mathrm{e,k}}}{\partial t} = -\gamma_{\mathrm{e}}\frac{\partial N_{\mathrm{e,k}}}{\partial x} + \mathcal{C}_{\mathrm{e}}\frac{\partial i_{\mathrm{e,k}}}{\partial x}, \qquad \mathrm{k} \in \{\mathrm{n,\ s,\ p}\}, \tag{3d}$$

$$N_{\mathrm{e,k}} = -\epsilon_{\mathrm{k}}^{\mathrm{b}} D_{\mathrm{e}}(c_{\mathrm{e,k}})\frac{\partial c_{\mathrm{e,k}}}{\partial x} + \frac{\mathcal{C}_{\mathrm{e}} t^{+}}{\gamma_{\mathrm{e}}} i_{\mathrm{e,k}}, \qquad \mathrm{k} \in \{\mathrm{n,\ s,\ p}\}, \tag{3e}$$

$$\mathcal{C}_{\mathrm{k}}\frac{\partial c_{\mathrm{s,k}}}{\partial t} = \frac{1}{r_{\mathrm{k}}^2}\frac{\partial}{\partial r_{\mathrm{k}}}\left(r_{\mathrm{k}}^2\frac{\partial c_{\mathrm{s,k}}}{\partial r_{\mathrm{k}}}\right), \qquad \mathrm{k} \in \{\mathrm{n,\ p}\}, \tag{3f}$$

Electrochemical reactions:

$$j_{\mathrm{k}} = j_{0,\mathrm{k}} \sinh\left(\frac{\eta_{\mathrm{k}}}{2}\right), \qquad \mathrm{k} \in \{\mathrm{n,\ p}\}, \tag{3g}$$

$$j_{0,\mathrm{k}} = \frac{\gamma_{\mathrm{k}}}{\mathcal{C}_{\mathrm{r,k}}} c_{\mathrm{s,k}}^{1/2}(1 - c_{\mathrm{k}})^{1/2} c_{\mathrm{e,k}}^{1/2}\big|_{r_{\mathrm{k}}=1}, \qquad \mathrm{k} \in \{\mathrm{n,\ p}\}, \tag{3h}$$

$$\eta_{\mathrm{k}} = \phi_{\mathrm{s,k}} - \phi_{\mathrm{e,k}} - U_{\mathrm{k}}(c_{\mathrm{s,k}}\big|_{r_{\mathrm{k}}=1}), \qquad \mathrm{k} \in \{\mathrm{n,\ p}\}, \tag{3i}$$

Boundary conditions

Current:

$$i_{\mathrm{e,n}}\big|_{x=0} = 0, \quad i_{\mathrm{e,p}}\big|_{x=1} = 0, \tag{4a}$$

$$\phi_{\mathrm{e,n}}\big|_{x=L_{\mathrm{n}}} = \phi_{\mathrm{e,s}}\big|_{x=L_{\mathrm{n}}}, \quad i_{\mathrm{e,n}}\big|_{x=L_{\mathrm{n}}} = i_{\mathrm{e,s}}\big|_{x=L_{\mathrm{n}}} = I, \tag{4b}$$

$$\phi_{\mathrm{e,s}}\big|_{x=1-L_{\mathrm{p}}} = \phi_{\mathrm{e,p}}\big|_{x=1-L_{\mathrm{p}}}, \quad i_{\mathrm{e,s}}\big|_{x=1-L_{\mathrm{p}}} = i_{\mathrm{e,p}}\big|_{x=1-L_{\mathrm{p}}} = I, \tag{4c}$$

Concentration in electrolyte:

$$N_{\mathrm{e,n}}\big|_{x=0} = 0, \quad N_{\mathrm{e,p}}\big|_{x=1} = 0, \tag{4d}$$

$$c_{\mathrm{e,n}}\big|_{x=L_{\mathrm{n}}} = c_{\mathrm{e,s}}|_{x=L_{\mathrm{n}}}, \quad N_{\mathrm{e,n}}\big|_{x=L_{\mathrm{n}}} = N_{\mathrm{e,s}}\big|_{x=L_{\mathrm{n}}}, \tag{4e}$$

$$c_{\mathrm{e,s}}|_{x=1-L_{\mathrm{p}}} = c_{\mathrm{e,p}}|_{x=1-L_{\mathrm{p}}}, \quad N_{\mathrm{e,s}}\big|_{x=1-L_{\mathrm{p}}} = N_{\mathrm{e,p}}\big|_{x=1-L_{\mathrm{p}}}, \tag{4f}$$

Concentration in the electrode active material:

$$\left.\frac{\partial c_{\mathrm{s,k}}}{\partial r_{\mathrm{k}}}\right|_{r_{\mathrm{k}}=0} = 0, \quad -\frac{a_{\mathrm{k}}\gamma_{\mathrm{k}}}{\mathcal{C}_{\mathrm{k}}}\left.\frac{\partial c_{\mathrm{s,k}}}{\partial r_{\mathrm{s,k}}}\right|_{r_{\mathrm{k}}=1} = j_{\mathrm{k}}, \quad \mathrm{k} \in \{\mathrm{n,\ p}\}, \tag{4g}$$

Reference potenital:

$$\phi_{\mathrm{s,n}}|_{x=0} = 0, \tag{4h}$$

Initial conditions

$$c_{\mathrm{s,k}}(x, r, 0) = c_{\mathrm{s,k,0}}, \qquad \mathrm{k} \in \{\mathrm{n,\ p}\}, \tag{4i}$$

$$c_{\mathrm{e,k}}(x, 0) = 1, \qquad \mathrm{k} \in \{\mathrm{n,\ s,\ p}\}. \tag{4j}$$

Before proceeding with model reduction, we note some of helpful relations. The terminal voltage is given by

$$V = \phi_{\mathrm{s,p}}\big|_{x=1} - \phi_{\mathrm{s,n}}\big|_{x=0}. \tag{5}$$

We can re-write this in a more useful form by considering a general path current follows through the cell. We consider the current entering through the negative current collector at $x = 0$ and then travelling through the negative electrode to a point $x_{\mathrm{n}} \in [0, L_{\mathrm{n}}]$, at this point an electrochemical reaction occurs so that the current is transferred into the electrolyte. The current then travels through the electrolyte until it reaches the point $x_{\mathrm{p}} \in [1 - L_{\mathrm{p}}, 1]$ where another electrochemical reaction occurs transferring the current into the positive electrode. Finally, the current travels through the positive electrode until it reaches the positive current collector. The terminal voltage can be written in terms of the potential drops associated with each section of this path as

$$\begin{aligned} V = \;& \phi_{\mathrm{s,n}}\big|_{x=x_{\mathrm{n}}} - \phi_{\mathrm{s,n}}\big|_{x=0} && \text{(Negative electrode)} \\ &+ \phi_{\mathrm{e,n}}\big|_{x=x_{\mathrm{n}}} - \phi_{\mathrm{s,n}}\big|_{x=x_{\mathrm{n}}} && \text{(Negative electrochemical reaction)} \\ &+ \phi_{\mathrm{e,p}}\big|_{x=x_{\mathrm{p}}} - \phi_{\mathrm{e,n}}\big|_{x=x_{\mathrm{n}}} && \text{(Electrolyte)} \\ &+ \phi_{\mathrm{s,p}}\big|_{x=x_{\mathrm{p}}} - \phi_{\mathrm{e,p}}\big|_{x=x_{\mathrm{p}}} && \text{(Positive electrochemical reaction)} \\ &+ \phi_{\mathrm{s,p}}\big|_{x=1} - \phi_{\mathrm{s,p}}\big|_{x=x_{\mathrm{p}}} && \text{(Positive electrode).} \end{aligned} \tag{6}$$

We define the pointwise open circuit voltage to be

$$U_{\mathrm{eq}}\big|_{x_{\mathrm{n}},x_{\mathrm{p}}} = U_{\mathrm{p}}(c_{\mathrm{s,p}}\big|_{r=1})\big|_{x=x_{\mathrm{p}}} - U_{\mathrm{n}}(c_{\mathrm{s,n}}\big|_{r=1})\big|_{x=x_{\mathrm{n}}} \tag{7}$$

and the pointwise solid phase ohmic losses to be

$$\Delta\Phi_{\mathrm{Solid}}\big|_{x_{\mathrm{n}},x_{\mathrm{p}}} = \left(\phi_{\mathrm{s,p}}\big|_{x=1} - \phi_{\mathrm{s,p}}\big|_{x=x_{\mathrm{p}}}\right) + \left(\phi_{\mathrm{s,n}}\big|_{x=x_{\mathrm{n}}} - \phi_{\mathrm{s,n}}\big|_{x=0}\right). \tag{8}$$

Then, using the definition of the reaction overpotential given in (3i), (6) becomes

$$V = U_{\mathrm{eq}}\big|_{x_{\mathrm{n}},x_{\mathrm{p}}} + \eta_{\mathrm{p}}\big|_{x=x_{\mathrm{p}}} - \eta_{\mathrm{n}}\big|_{x=x_{\mathrm{n}}} + \phi_{\mathrm{e,p}}\big|_{x=x_{\mathrm{p}}} - \phi_{\mathrm{e,n}}\big|_{x=x_{\mathrm{n}}} + \Delta\Phi_{\mathrm{Solid}}\big|_{x_{\mathrm{n}},x_{\mathrm{p}}}. \tag{9}$$

Equation (9) provides the voltages in terms the internal pointwise OCV, ohmic losses, and overpotentials of a particular current path through the cell. However, we can also express the voltage in terms of the average OCV, ohmic losses, and overpotentials by electrode-averaging (9). This is done by integrating (9) with respect to $x_{\mathrm{n}} \in [0, L_{\mathrm{n}}]$ and dividing by the negative electrode thickness, L_{n}, and then integrating with respect to $x_{\mathrm{p}} \in [1 - L_{\mathrm{p}}, 1]$ and dividing by the positive electrode thickness, L_{p}. The result is

$$V = \overline{U}_{\mathrm{eq}} + \overline{\eta}_{\mathrm{p}} - \overline{\eta}_{\mathrm{n}} + \overline{\phi}_{\mathrm{e,p}} - \overline{\phi}_{\mathrm{e,n}} + \overline{\Delta\Phi_{\mathrm{Solid}}}. \tag{10}$$

where we use an overbar to represent the operation

$$\bar{\cdot} := \frac{1}{L_{\mathrm{p}}} \int_{1}^{1-L_{\mathrm{p}}} \left(\frac{1}{L_{\mathrm{n}}} \int_{0}^{L_{\mathrm{n}}} \cdot \, \mathrm{d}x_{\mathrm{n}} \right) \mathrm{d}x_{\mathrm{p}}. \tag{11}$$

It is this electrode-averaged form of the voltage expression which will play a central role in our extension of the single particle model. Without this electrode-averaged form, the extended

model would need to be more complex than the model we present in order to obtain the same degree of accuracy.

Another useful property can be found by integrating (3d) with respect to x over Ω_{k} for each $\mathrm{k} \in \{\mathrm{n}, \mathrm{s}, \mathrm{p}\}$, applying the boundary conditions (4a), (4b), (4c), (4d), (4e), (4f), and applying the initial condition (4j), to obtain

$$\int_0^{L_{\mathrm{n}}} c_{\mathrm{e,n}}\, dx + \int_{L_{\mathrm{n}}}^{1-L_{\mathrm{p}}} c_{\mathrm{e,s}}\, dx + \int_{1-L_{\mathrm{p}}}^{1} c_{\mathrm{e,p}}\, dx = 1, \tag{12}$$

that is, the total number of lithium ions in the electrolyte is fixed for all time.

3.2. The limit $\mathcal{C}_e \to 0$

We consider the limit of high electrical conductivity in the electrodes and electrolyte and fast migration of lithium ions in the electrolyte relative to the discharge time. To do this, we consider the limit $\mathcal{C}_{\mathrm{e}} \to 0$, where $\mathcal{C}_{\mathrm{e}}$ is the ratio of the typical timescale for lithium ion diffusion to the typical discharge timescale, $\sigma_{\mathrm{k}} \to \infty$, where σ_{k} is ratio of the thermal voltage to the typical ohmic drop in the solid, and $\hat{\kappa}_{\mathrm{e}} \to \infty$, where $\hat{\kappa}_{\mathrm{e}}$ is the ratio of the thermal voltage to the typical ohmic drop in the electrolyte. We take the distinguished limit in which $\sigma_{\mathrm{k}}\mathcal{C}_{\mathrm{e}}$ and $\hat{\kappa}_{\mathrm{e}}\mathcal{C}_{\mathrm{e}}$ both tend to a constant as $\mathcal{C}_{\mathrm{e}} \to 0$, $\sigma_{\mathrm{k}} \to \infty$, and $\hat{\kappa}_{\mathrm{e}} \to \infty$ by setting

$$\sigma_{\mathrm{k}} = \frac{\sigma'_{\mathrm{k}}}{\mathcal{C}_{\mathrm{e}}}, \quad \sigma'_{\mathrm{k}} = \mathcal{O}(1), \quad \mathrm{k} \in \{\mathrm{n}, \mathrm{p}\},$$
$$\hat{\kappa}_{\mathrm{e}} = \frac{\hat{\kappa}'_{\mathrm{e}}}{\mathcal{C}_{\mathrm{e}}}, \quad \hat{\kappa}'_{\mathrm{e}} = \mathcal{O}(1),$$

we then expand all variables in powers of $\mathcal{C}_{\mathrm{e}}$ as

$$c_{\mathrm{s,k}} \sim c^0_{\mathrm{s,k}} + \mathcal{C}_{\mathrm{e}} c^1_{\mathrm{s,k}} + \mathcal{C}^2_{\mathrm{e}} c^2_{\mathrm{s,k}} + \ldots,$$

etc.

3.2.1. Leading-order model

At leading order in $\mathcal{C}_{\mathrm{e}}$, (3d) and (3e) are

$$\frac{\partial N^0_{\mathrm{e,k}}}{\partial x} = 0, \quad N^0_{\mathrm{e,k}} = -D_{\mathrm{e}}(c^0_{\mathrm{e,k}}) \frac{\partial c^0_{\mathrm{e,k}}}{\partial x}, \quad \mathrm{k} \in \{\mathrm{n}, \mathrm{s}, \mathrm{p}\}, \tag{13}$$

which, upon application of the leading-order boundary conditions (4d), (4e), (4f), the leading-order initial condition (4j), and the leading-order component of the condition (12), yield

$$N^0_{\mathrm{e,k}} = 0, \quad c^0_{\mathrm{e,k}} = 1, \quad \mathrm{k} \in \{\mathrm{n}, \mathrm{s}, \mathrm{p}\}. \tag{14}$$

Thus there is no depletion of the electrolyte at leading order. Equations (3b) and (3c), at leading order in $\mathcal{C}_{\mathrm{e}}$, are then

$$\frac{\partial \phi^0_{\mathrm{e,k}}}{\partial x} = 0, \quad \frac{\partial \phi^0_{\mathrm{s,k}}}{\partial x} = 0. \tag{15}$$

Since $c^0_{\mathrm{e,k}}$, $\phi^0_{\mathrm{e,k}}$, and $\phi^0_{\mathrm{s,k}}$ are all independent of x and $c^0_{\mathrm{s,k}}$ is initially independent of x, it follows from the leading order components of (3g), (3h), and (3i), that j^0_{k}, $j^0_{0,\mathrm{k}}$ and η^0_{k} do not

depend on x. Therefore, we integrate (3a) with respect to x over Ω_{k} for $\mathrm{k} = \mathrm{n}, \mathrm{p}$ and apply (4a), (4b), (4c), to obtain

$$i^0_{\mathrm{e,n}} = \frac{xI}{L_{\mathrm{n}}}, \quad i^0_{\mathrm{e,s}} = I, \quad i^0_{\mathrm{e,p}} = \frac{(1-x)I}{L_{\mathrm{p}}}, \tag{16}$$

$$j^0_{\mathrm{n}} = \frac{I}{L_{\mathrm{n}}}, \quad j^0_{\mathrm{p}} = -\frac{I}{L_{\mathrm{p}}}. \tag{17}$$

From the leading order component of (3g), we then have

$$\eta^0_{\mathrm{n}} = 2\sinh^{-1}\left(\frac{I}{j^0_{0,\mathrm{n}} L_{\mathrm{n}}}\right), \quad \eta^0_{\mathrm{p}} = -2\sinh^{-1}\left(\frac{I}{j^0_{0,\mathrm{p}} L_{\mathrm{p}}}\right). \tag{18}$$

Employing (15) in conjunction with the leading order interior boundary conditions (4b) and (4c), we obtain

$$\phi^0_{\mathrm{e,p}} - \phi^0_{\mathrm{e,n}} = 0, \tag{19}$$

so, to leading order, there is no potential drop in the electrolyte (for both the pointwise and electrode averaged cases). From (15), we also have that there are no solid phase ohmic losses (for both the pointwise and electrode-averaged cases) at leading order.

We are now in position to summarise the leading-order model. The leading-order description of lithium in the electrode particles is given by taking the leading-order component of (3f) and inserting (17) into the leading-order component of (4g) to obtain

$$\mathcal{C}_{\mathrm{k}} \frac{\partial c^0_{\mathrm{s,k}}}{\partial t} = \frac{1}{r^2_{\mathrm{k}}} \frac{\partial}{\partial r_{\mathrm{k}}} \left(r^2_{\mathrm{k}} \frac{\partial c^0_{\mathrm{s,k}}}{\partial r_{\mathrm{k}}} \right), \qquad \mathrm{k} \in \{\mathrm{n}, \mathrm{p}\} \tag{20a}$$

$$\left.\frac{\partial c^0_{\mathrm{s,k}}}{\partial r_{\mathrm{k}}}\right|_{r_{\mathrm{k}}=0} = 0, \quad -\frac{a_{\mathrm{k}}\gamma_{\mathrm{k}}}{\mathcal{C}_{\mathrm{k}}} \left.\frac{\partial c^0_{\mathrm{s,k}}}{\partial r_{\mathrm{k}}}\right|_{r_{\mathrm{k}}=1} = \begin{cases} \frac{I}{L_{\mathrm{n}}}, & \mathrm{k} = \mathrm{n}, \\ -\frac{I}{L_{\mathrm{p}}}, & \mathrm{k} = \mathrm{p}, \end{cases} \qquad \mathrm{k} \in \{\mathrm{n}, \mathrm{p}\} \tag{20b}$$

$$c^0_{\mathrm{s,k}}(r_{\mathrm{k}}, 0) = c_{\mathrm{s,k},0}, \qquad \mathrm{k} \in \{\mathrm{n}, \mathrm{p}\}, \tag{20c}$$

Since $c^0_{\mathrm{s,k}}$ is independent of x, the leading-order electrode-averaged OCV is simply

$$\overline{U}^0_{\mathrm{eq}} = U_{\mathrm{p}}(c^0_{\mathrm{s,p}}\big|_{r_{\mathrm{p}}=1}) - U_{\mathrm{n}}(c^0_{\mathrm{s,n}}\big|_{r_{\mathrm{n}}=1}) \tag{20d}$$

Additionally, the leading-order electrode-averaged reaction overpotentials are just $\overline{\eta}^0_{\mathrm{k}} = \eta^0_{\mathrm{k}}$. Therefore, the leading-order voltage is given by

$$V^0 = \underbrace{U_{\mathrm{p}}(c^0_{\mathrm{s,p}})\big|_{r_{\mathrm{p}}=1} - U_{\mathrm{n}}(c^0_{\mathrm{s,n}})\big|_{r_{\mathrm{n}}=1}}_{\text{Open Circuit Voltage}} \underbrace{- 2\sinh^{-1}\left(\frac{I}{j^0_{0,\mathrm{p}} L_{\mathrm{p}}}\right) - 2\sinh^{-1}\left(\frac{I}{j^0_{0,\mathrm{n}} L_{\mathrm{n}}}\right)}_{\text{Reaction Overpotentials}} \tag{20e}$$

where the leading order component of the exchange current density, as given by (3h), is

$$j^0_{0,\mathrm{k}} = \frac{\gamma_{\mathrm{k}}}{\mathcal{C}_{\mathrm{r,k}}} (c^0_{\mathrm{s,k}})^{1/2} (1 - c^0_{\mathrm{s,k}})^{1/2}. \tag{20f}$$

We identify (20) as the dimensionless form of the single particle model (SPM) [15, 27]. The name refers to the requirement to only solve a diffusion equation for one particle in each

electrode, rather than for many particles as in the DFN model. This model should not be interpreted as replacing the many particles in an electrode by a single particle. Instead, in this limit all the particles in an electrode behave in exactly the same way and it is therefore sufficient to solve for just one representative particle.

3.2.2. First-order correction

We now proceed to calculate the $\mathcal{O}(\mathcal{C}_\mathrm{e})$ corrections terms, which will extend the range of applicability of the SPM to higher C-rates. At $\mathcal{O}(\mathcal{C}_\mathrm{e})$, (3d) and (3e) become

$$\frac{\partial N^1_{\mathrm{e,k}}}{\partial x} = \frac{1}{\gamma_\mathrm{e}} \frac{\partial i^0_{\mathrm{e,k}}}{\partial x}, \qquad \mathrm{k} \in \{\mathrm{n},\, \mathrm{p}\}, \tag{21}$$

$$N^1_{\mathrm{e,k}} = -\epsilon^b_\mathrm{k} D_\mathrm{e}(c^0_{\mathrm{e,k}}) \frac{\partial c^1_{\mathrm{e,k}}}{\partial x} + \frac{t^+}{\gamma_\mathrm{e}} i^0_{\mathrm{e,k}}, \qquad \mathrm{k} \in \{\mathrm{n},\, \mathrm{p}\}. \tag{22}$$

Integrating (21) with respect to x over Ω_k for each $\mathrm{k} \in \{\mathrm{n},\, \mathrm{s},\, \mathrm{p}\}$ and applying the $\mathcal{O}(\mathcal{C}_\mathrm{e})$ components of the boundary conditions (4d), (4e), and (4f), we obtain

$$N_{\mathrm{e,n}} = \frac{Ix}{\gamma_\mathrm{e} L_\mathrm{n}}, \quad N_{\mathrm{e,s}} = \frac{I}{\gamma_\mathrm{e}}, \quad N_{\mathrm{e,p}} = \frac{I(1-x)}{\gamma_\mathrm{e} L_\mathrm{p}}. \tag{23}$$

We substitute (23) into (22) and then integrate with respect to x over Ω_k for each $\mathrm{k} \in \{\mathrm{n},\, \mathrm{s},\, \mathrm{p}\}$ using the $\mathcal{O}(\mathcal{C}_\mathrm{e})$ components of the interior boundary conditions (4e) (4f) and fixed lithium ion condition (12) to determine the constants of integration. From this, we get

$$c^1_{\mathrm{e,n}} = \frac{(1-t^+)I}{\gamma_\mathrm{e} 6 D_\mathrm{e}(1)} \left(2\left(\frac{L_\mathrm{p}^2}{\epsilon^b_\mathrm{p}} - \frac{L_\mathrm{n}^2}{\epsilon^b_\mathrm{n}} \right) + \frac{3L_s}{\epsilon^b_\mathrm{s}}(1 + L_\mathrm{p} - L_\mathrm{n}) + \frac{3}{\epsilon^b_\mathrm{n} L_\mathrm{n}}(L_\mathrm{n}^2 - x^2) \right), \tag{24a}$$

$$c^1_{\mathrm{e,p}} = \frac{(1-t^+)I}{6\gamma_\mathrm{e} D_\mathrm{e}(1)} \left(2\left(\frac{L_\mathrm{p}^2}{\epsilon^b_\mathrm{p}} - \frac{L_\mathrm{n}^2}{\epsilon^b_\mathrm{n}} \right) + \frac{3}{\epsilon^b_\mathrm{s}}(L_\mathrm{n}^2 - L_\mathrm{p}^2 + 1 - 2x) \right), \tag{24b}$$

$$c^1_{\mathrm{e,p}} = \frac{(1-t^+)I}{6\gamma_\mathrm{e} D_\mathrm{e}(1)} \left(2\left(\frac{L_\mathrm{p}^2}{\epsilon^b_\mathrm{p}} - \frac{L_\mathrm{n}^2}{\epsilon^b_\mathrm{n}} \right) + \frac{3L_s}{\epsilon^b_\mathrm{s}}(L_\mathrm{p} - L_\mathrm{n} - 1) + \frac{3}{L_\mathrm{p}\epsilon^b_\mathrm{p}}((x-1)^2 - L_\mathrm{p}^2) \right). \tag{24c}$$

At $\mathcal{O}(\mathcal{C}_\mathrm{e})$, (3b) becomes

$$i^0_{\mathrm{e,k}} = \epsilon^b_\mathrm{k} \hat{\kappa}'_\mathrm{e} \kappa_\mathrm{e}(1) \left(-\frac{\partial \phi^1_{\mathrm{e,k}}}{\partial x} + 2(1-t^+) \frac{\partial c^1_{\mathrm{e,k}}}{\partial x} \right). \tag{25}$$

We substitute (16) into (25), integrate with respect to x over Ω_k for each $\mathrm{k} \in \{\mathrm{n},\, \mathrm{s},\, \mathrm{p}\}$ and determine two of the three constants of integration by applying the $\mathcal{O}(\mathcal{C}_\mathrm{e})$ components of the interior boundary conditions (4b) and (4f) to obtain

$$\phi^1_{\mathrm{e,n}} = \tilde{\phi}_\mathrm{e} + 2(1-t^+)c^1_{\mathrm{e,n}} - \frac{I}{\hat{\kappa}'_\mathrm{e}\kappa_\mathrm{e}(1)} \left(\frac{x^2 - L_\mathrm{n}^2}{2\epsilon^b_\mathrm{n} L_\mathrm{n}} + \frac{L_\mathrm{n}}{\epsilon^b_\mathrm{s}} \right), \tag{26a}$$

$$\phi^1_{\mathrm{e,s}} = \tilde{\phi}_\mathrm{e} + 2(1-t^+)c^1_{\mathrm{e,s}} - \frac{Ix}{\hat{\kappa}'_\mathrm{e}\kappa_\mathrm{e}(1)\epsilon^b_\mathrm{s}}, \tag{26b}$$

$$\phi^1_{\mathrm{e,n}} = \tilde{\phi}_\mathrm{e} + 2(1-t^+)c^1_{\mathrm{e,p}} - \frac{I}{\hat{\kappa}'_\mathrm{e}\kappa_\mathrm{e}(1)} \left(\frac{x(2-x) + L_\mathrm{p}^2 - 1}{2\epsilon^b_\mathrm{p} L_\mathrm{p}} + \frac{1 - L_\mathrm{p}}{\epsilon^b_\mathrm{s}} \right), \tag{26c}$$

where $\tilde{\phi}_{\mathrm{e}}$ is constant, the form of which is provided in Appendix A.

At $\mathcal{O}(\mathcal{C}_{\mathrm{e}})$, (3c) is

$$I - i^0_{\mathrm{e,k}} = -\sigma'_{\mathrm{k}} \frac{\partial \phi^1_{\mathrm{k}}}{\partial x}, \quad \mathrm{k} \in \{\mathrm{n},\, \mathrm{p}\}, \tag{27}$$

which upon using (16) and integrating with respect to x, gives

$$\phi^1_{\mathrm{s,n}} = \phi_{\mathrm{s,n}}\big|_{x=0} + \frac{Ix}{2\sigma'_{\mathrm{n}} L_{\mathrm{n}}} \left(2L_{\mathrm{n}} - x\right), \tag{28a}$$

$$\phi^1_{\mathrm{s,p}} = \phi_{\mathrm{s,p}}\big|_{x=1} + \frac{I(x-1)(1-2L_{\mathrm{p}}-x)}{2\sigma'_{\mathrm{p}} L_{\mathrm{p}}}. \tag{28b}$$

At $\mathcal{O}(\mathcal{C}_{\mathrm{e}})$, (3a), (4a), (4b), and (4c) give

$$\frac{\partial i^1_{\mathrm{e,k}}}{\partial x} = j^1_{\mathrm{k}}, \qquad \mathrm{k} \in \{\mathrm{n},\, \mathrm{p}\} \tag{29a}$$

$$i^1_{\mathrm{e,n}}\big|_{x=0,L_{\mathrm{n}}} = i^1_{\mathrm{e,p}}\big|_{1-L_{\mathrm{p}},1} = 0. \tag{29b}$$

Here we approach a key step in our derivation. Integrating (29a) with respect to x over Ω_{k} for $\mathrm{k} \in \{\mathrm{n},\, \mathrm{p}\}$ and applying (29b) gives the conditions

$$\int_0^{L_{\mathrm{n}}} j^1_{\mathrm{n}} \,\mathrm{d}x = 0, \quad \int_{1-l_{\mathrm{p}}}^{1} j^1_{\mathrm{p}} \,\mathrm{d}x = 0. \tag{30}$$

Thus the electrode-averaged corrections to the reaction currents j_{n} and j_{p} are zero. This means that after averaging the $\mathcal{O}(\mathcal{C}_{\mathrm{e}})$ components of (3f) and (4g) in x over Ω_{k} for each $\mathrm{k} \in \{\mathrm{n},\, \mathrm{p}\}$ and using (30), we get

$$\mathcal{C}_{\mathrm{k}} \frac{\partial \overline{c}^1_{\mathrm{s,k}}}{\partial t} = \frac{1}{r_{\mathrm{k}}^2} \frac{\partial}{\partial r_{\mathrm{k}}} \left(r_{\mathrm{k}}^2 \frac{\partial \overline{c}^1_{\mathrm{s,k}}}{\partial r_{\mathrm{k}}} \right), \qquad \mathrm{k} \in \{\mathrm{n},\, \mathrm{p}\}, \tag{31a}$$

$$\left.\frac{\partial \overline{c}^1_{\mathrm{s,k}}}{\partial r_{\mathrm{k}}}\right|_{r_{\mathrm{k}}=0} = \left.\frac{\partial \overline{c}^1_{\mathrm{s,k}}}{\partial r_{\mathrm{k}}}\right|_{r_{\mathrm{k}}=1} = 0, \qquad \mathrm{k} \in \{\mathrm{n},\, \mathrm{p}\}, \tag{31b}$$

$$\overline{c}^1_{\mathrm{s,k}}(r_{\mathrm{k}}, 0) = 0, \qquad \mathrm{k} \in \{\mathrm{n},\, \mathrm{p}\}. \tag{31c}$$

where crucially, there is no average flux on the surface $r_{\mathrm{k}} = 1$. The solution to (31) is therefore simply

$$\overline{c}^1_{\mathrm{s,n}} = 0, \quad \overline{c}^1_{\mathrm{s,p}} = 0. \tag{32}$$

Therefore, the $\mathcal{O}(\mathcal{C}_{\mathrm{e}})$ component of the electrode-averaged OCV is

$$\overline{U}^1_{\mathrm{eq}} = U'_{\mathrm{p}}(c^0_{\mathrm{s,p}})\overline{c}^1_{\mathrm{s,p}} - U'_{\mathrm{n}}(c^0_{\mathrm{s,n}})\overline{c}^1_{\mathrm{s,n}} = 0. \tag{33}$$

The $\mathcal{O}(\mathcal{C}_{\mathrm{e}})$ components of (3g), (3i), and (3h) are

$$j^1_{\mathrm{k}} = j^1_{0,\mathrm{k}} \sinh\left(\frac{\eta^0_{\mathrm{k}}}{2}\right) + \frac{j^0_{0,\mathrm{k}} \eta^1_{\mathrm{k}}}{2} \cosh\left(\frac{\eta^0_{\mathrm{k}}}{2}\right), \tag{34a}$$

$$\eta^1_{\mathrm{k}} = \phi^1_{\mathrm{s,k}} - \phi^1_{\mathrm{e,k}} - U'_{\mathrm{k}}(c^0_{\mathrm{s,k}}) c^1_{\mathrm{s,k}}\big|_{r_{\mathrm{k}}=1}, \tag{34b}$$

$$j^1_{0,\mathrm{k}} = \frac{j^0_{0,\mathrm{k}}}{2} \left(\frac{c^1_{\mathrm{s,k}}}{c^0_{\mathrm{s,k}}} - \frac{c^1_{\mathrm{s,k}}}{1 - c^0_{\mathrm{s,k}}} + c^1_{\mathrm{e,k}} \right) \Bigg|_{r_{\mathrm{k}}=1} \tag{34c}$$

where η_{k}^0 and $j_{0,\mathrm{k}}^0$ are given by (18) and (20f), respectively. Averaging (34a) over electrode Ω_{k}, gives

$$\overline{\eta}_{\mathrm{k}}^1 = -\overline{c}_{\mathrm{e,k}}^1 \tanh\left(\frac{\eta_{\mathrm{k}}^0}{2}\right) = \frac{\overline{c}_{\mathrm{e,k}}^1 I}{\sqrt{(j_{0,k}^0 L_k)^2 + I^2}}. \tag{35}$$

We can also easily obtain $\overline{\phi}_{\mathrm{e,k}}^1$ and $\overline{\phi}_{\mathrm{s,k}}^1$ by electrode-averaging (26) and (28). The expressions for these can be found in Appendix A.

We now have all the components necessary to obtain the first-order correction to the voltage. Inserting (33), (35), and the electrode-averaged potential expressions in Appendix A into (10), we obtain

$$\begin{aligned} V^1 = &\left(\frac{\overline{c}_{\mathrm{e,p}} I}{\sqrt{(j_{0,\mathrm{p}}^0 L_{\mathrm{p}})^2 + I^2}} + \frac{\overline{c}_{\mathrm{e,n}} I}{\sqrt{(j_{0,\mathrm{n}}^0 L_{\mathrm{n}})^2 + I^2}}\right) + 2(1-t^+)\left(\overline{c}_{\mathrm{e,p}}^1 - \overline{c}_{\mathrm{e,n}}^1\right) \\ &- \frac{I}{\hat{\kappa}_{\mathrm{e}}' \kappa_{\mathrm{e}}(1)}\left(\frac{L_{\mathrm{n}}}{3\epsilon_{\mathrm{n}}^b} + \frac{L_{\mathrm{s}}}{\epsilon_{\mathrm{s}}^b} + \frac{L_{\mathrm{p}}}{3\epsilon_{\mathrm{p}}^b}\right) - \frac{I}{3}\left(\frac{L_{\mathrm{p}}}{\tilde{\sigma}_{\mathrm{p}}} + \frac{L_{\mathrm{n}}}{\tilde{\sigma}_{\mathrm{n}}}\right). \end{aligned} \tag{36}$$

This is a purely algebraic expression, so that we have improved the accuracy of the leading order expression for V (i.e. the SPM) at negligible additional computational expense. The first term of (36) corresponds to corrections to the reaction overpotentials due to concentration variations in the electrolyte, the second to the concentration overpotential, the third to electrolyte Ohmic losses, and the fourth to solid phase Ohmic losses.

3.3. Combined voltage expression

To write an expression for the combined leading-order and first-order voltage, $V = V^0 + \mathcal{C}_{\mathrm{e}} V^1$, we define the electrode-averaged exchange current densities to be

$$\overline{j}_{0,\mathrm{n}} = \frac{1}{L_{\mathrm{n}}}\int_0^{L_{\mathrm{n}}} \frac{\gamma_{\mathrm{n}}}{\mathcal{C}_{\mathrm{r,n}}}(c_{\mathrm{s,n}}^0)^{1/2}(1-c_{\mathrm{s,n}}^0)^{1/2}(1+\mathcal{C}_{\mathrm{e}} c_{\mathrm{e,n}}^1)^{1/2}\,\mathrm{d}x, \tag{37a}$$

$$\overline{j}_{0,\mathrm{p}} = \frac{1}{L_{\mathrm{p}}}\int_{1-L_{\mathrm{p}}}^{1} \frac{\gamma_{\mathrm{p}}}{\mathcal{C}_{\mathrm{r,p}}}(c_{\mathrm{s,p}}^0)^{1/2}(1-c_{\mathrm{s,p}}^0)^{1/2}(1+\mathcal{C}_{\mathrm{e}} c_{\mathrm{e,p}}^1)^{1/2}\,\mathrm{d}x, \tag{37b}$$

and use the fact that

$$-2\sinh^{-1}\left(\frac{I}{\overline{j}_{0,\mathrm{k}} L_{\mathrm{k}}}\right) = -2\sinh^{-1}\left(\frac{I}{j_{0,\mathrm{k}}^0 L_{\mathrm{k}}}\right) + \mathcal{C}_{\mathrm{e}}\frac{\overline{c}_{\mathrm{e,k}}^1 I}{\lambda\sqrt{(j_{0,\mathrm{k}}^0 L_{\mathrm{k}})^2 + I^2}} + \mathcal{O}\left(\mathcal{C}_{\mathrm{e}}^2\right).$$

The combined leading-order and first-order electrode-averaged components of the voltage expression are then given as

$$\overline{U}_{\mathrm{eq}} = U_{\mathrm{p}}(c_{\mathrm{s,p}}^0\big|_{r_{\mathrm{p}}=1}) - U_{\mathrm{n}}(c_{\mathrm{s,n}}^0\big|_{r_{\mathrm{n}}=1}) \tag{38a}$$

$$\overline{\eta}_{\mathrm{r}} = -2\sinh^{-1}\left(\frac{I}{\overline{j}_{\mathrm{p}} L_{\mathrm{n}}}\right) - 2\sinh^{-1}\left(\frac{I}{\overline{j}_{\mathrm{n}} L_{\mathrm{n}}}\right). \tag{38b}$$

$$\overline{\eta}_{\mathrm{c}} = 2\mathcal{C}_{\mathrm{e}}(1-t^+)\left(\overline{c}_{\mathrm{e,p}}^1 - \overline{c}_{\mathrm{e,n}}^1\right) \tag{38c}$$

$$\overline{\Delta\Phi}_{\mathrm{Elec}} = -\frac{I}{\hat{\kappa}_{\mathrm{e}}\kappa_{\mathrm{e}}(1)}\left(\frac{L_{\mathrm{n}}}{3\epsilon_{\mathrm{n}}^b} + \frac{L_{\mathrm{s}}}{\epsilon_{\mathrm{s}}^b} + \frac{L_{\mathrm{p}}}{3\epsilon_{\mathrm{p}}^b}\right), \tag{38d}$$

$$\overline{\Delta\Phi}_{\mathrm{Solid}} = -\mathcal{C}_{\mathrm{e}}(\overline{\varphi}_{\mathrm{s,p}}^1 - \overline{\phi}_{\mathrm{s,n}}^1), \tag{38e}$$

respectively. The combined voltage accurate to $\mathcal{O}\left(\mathcal{C}_{\mathrm{e}}^{2}\right)$ is then

$$V = \overline{U}_{\mathrm{eq}} + \overline{\eta}_{\mathrm{r}} + \overline{\eta}_{\mathrm{c}} + \overline{\Delta\Phi}_{\mathrm{Elec}} + \overline{\Delta\Phi}_{\mathrm{Solid}}. \tag{39}$$

We refer to this model with the first-order corrected voltage as the SPMe(S), that is, the single particle model with electrolyte. The (S) refers to the fact that this formulation considers the electrolyte to be in steady state.

Before proceeding, we would like to draw further attention to what we view as the key step in the derivation of the SPMe(S), namely the electrode averaging step. Electrode averaging is essential as it provides us with a well-defined problem: given the electrode-averaged current, find the electrode-averaged potential differences. If instead we try to evaluate the pointwise voltage expression, we must determine both the current (since we only know the electrode-averaged current) and potential difference at a particular point. To get around this issue, it is typical for ad-hoc models in the literature, which use a pointwise voltage expression, to implicitly assume that the current at a particular point is equal to the electrode-averaged current. This is not in general true, since it implies that the concentrations in every particle of the DFN model would be the same across all operating conditions. Of course, this is not a bad first assumption to make in the limit we have been considering, and it is indeed valid for very low currents; this is the reason the SPM is a reasonable approximation. However, we have shown systemically that this assumption is only true at leading order and not at first order in our asymptotic expansion. Electrode averaging removes the requirement for this assumption, and ensures our expressions are also valid at first order, so we gain additional accuracy over the ad-hoc models for negligible additional computational cost.

4. Canonical SPMe

The SPMe(S) holds for cases where the electrolyte can be taken to be in quasi steady state (e.g. when the current varies over a longer timescale than the electrolyte diffusion timescale). However, for many applications transient effects in the electrolyte are important, particularly after a step change in current. These transient effects occur on the timescale of migration of lithium-ions in the electrolyte. To include these effects it is therefore natural to scale time with the timescale for migration of lithium ions, $t^{*} = \tau_{\mathrm{e}}\tilde{t}$. In this diffusion-timescale problem, at leading and first order the concentrations in the electrode particles remain constant and the source/sink terms in the electrolyte equation do not appear. We do not present the corresponding systematic asymptotic analysis for this diffusion-timescale problem here but instead simply state the composite model which produces the correct result on both the diffusion and discharge timescales. The main difference with the SPMe(S) is that we must now solve a PDE to obtain the first-order correction for the electrolyte concentration, $c_{\mathrm{e,k}}^{1}$. We shall take this model to be the canonical SPMe and therefore simply refer to it as the SPMe. The SPMe is summarised as

Governing Equations

$$\mathcal{C}_{\mathrm{k}}\frac{\partial c^0_{\mathrm{s,k}}}{\partial t} = -\frac{1}{r^2_{\mathrm{k}}}\frac{\partial}{\partial r_{\mathrm{k}}}\left(r^2_{\mathrm{k}}\frac{\partial c^0_{\mathrm{s,k}}}{\partial r_{\mathrm{k}}}\right), \qquad \mathrm{k}\in\{\mathrm{n},\,\mathrm{p}\}, \quad (40a)$$

$$\mathcal{C}_{\mathrm{e}}\epsilon_{\mathrm{k}}\gamma_{\mathrm{e}}\frac{\partial c^1_{\mathrm{e,k}}}{\partial t} = -\gamma_{\mathrm{e}}\frac{\partial N^1_{\mathrm{e,k}}}{\partial x} + \begin{cases} \frac{I}{L_{\mathrm{n}}}, & \mathrm{k}=\mathrm{n} \\ 0, & \mathrm{k}=\mathrm{s} \\ -\frac{I}{L_{\mathrm{p}}}, & \mathrm{k}=\mathrm{p} \end{cases} \qquad \mathrm{k}\in\{\mathrm{n},\,\mathrm{s},\,\mathrm{p}\}, \quad (40b)$$

$$N^1_{\mathrm{e,k}} = -\epsilon^{\mathrm{b}}_{\mathrm{k}}D_{\mathrm{e}}(1)\frac{\partial c^1_{\mathrm{e,k}}}{\partial x} + \begin{cases} \frac{xt^+I}{\gamma_{\mathrm{e}}L_{\mathrm{n}}}, & \mathrm{k}=\mathrm{n} \\ \frac{t^+I}{\gamma_{\mathrm{e}}}, & \mathrm{k}=\mathrm{s} \\ \frac{(1-x)t^+I}{\gamma_{\mathrm{e}}L_{\mathrm{p}}}, & \mathrm{k}=\mathrm{p} \end{cases} \qquad \mathrm{k}\in\{\mathrm{n},\,\mathrm{s},\,\mathrm{p}\}, \quad (40c)$$

Boundary Conditions

$$\left.\frac{\partial c^0_{\mathrm{s,k}}}{\partial r_{\mathrm{k}}}\right|_{r_{\mathrm{k}}=0} = 0, \quad -\frac{a_{\mathrm{k}}\gamma_k}{\mathcal{C}_k}\left.\frac{\partial c^0_{\mathrm{s,k}}}{\partial r_{\mathrm{k}}}\right|_{r_{\mathrm{k}}=1} = \begin{cases} \frac{I}{L_{\mathrm{n}}} & \mathrm{k}=\mathrm{n} \\ -\frac{I}{L_{\mathrm{p}}} & \mathrm{k}=\mathrm{p} \end{cases} \qquad \mathrm{k}\in\{\mathrm{n},\,\mathrm{p}\}, \quad (40d)$$

$$N^1_{\mathrm{e,n}}\big|_{x=0} = 0, \quad N^1_{\mathrm{e,p}}\big|_{x=1} = 0, \quad (40e)$$

$$c^1_{\mathrm{e,n}}|_{x=L_{\mathrm{n}}} = c^1_{\mathrm{e,s}}|_{x=L_{\mathrm{n}}}, \quad N^1_{\mathrm{e,n}}\big|_{x=L_{\mathrm{n}}} = N^1_{\mathrm{e,s}}\big|_{x=L_{\mathrm{n}}}, \quad (40f)$$

$$c^1_{\mathrm{e,s}}|_{x=1-L_{\mathrm{p}}} = c^1_{\mathrm{e,p}}|_{x=1-L_{\mathrm{p}}}, \quad N^1_{\mathrm{e,s}}\big|_{x=1-L_{\mathrm{p}}} = N^1_{\mathrm{e,p}}\big|_{x=1-L_{\mathrm{p}}}. \quad (40g)$$

Initial Conditions

$$c^0_{\mathrm{s,k}}(r_{\mathrm{k}},0) = c_{\mathrm{k},0} \qquad \mathrm{k}\in\{\mathrm{n},\,\mathrm{p}\}, \quad (40h)$$

$$c^1_{\mathrm{e,k}}(x,0) = 0 \qquad \mathrm{k}\in\{\mathrm{n},\,\mathrm{s},\,\mathrm{p}\}, \quad (40i)$$

Terminal Voltage

$$V = \overline{U}_{\mathrm{eq}} + \overline{\eta}_r + \overline{\eta}_c + \overline{\Delta\Phi}_{\mathrm{Elec}} + \overline{\Delta\Phi}_{\mathrm{Solid}}, \quad (40j)$$

where

$$\overline{U}_{\mathrm{eq}} = U_{\mathrm{p}}(c^0_{\mathrm{s,p}})\big|_{r_{\mathrm{p}}=1} - U_{\mathrm{n}}(c^0_{\mathrm{s,n}})\big|_{r_{\mathrm{n}}=1}, \quad (40k)$$

$$\overline{\eta}_r = -2\sinh^{-1}\left(\frac{I}{\overline{j}_{0,\mathrm{p}}L_{\mathrm{p}}}\right) - 2\sinh^{-1}\left(\frac{I}{\overline{j}_{0,\mathrm{n}}L_{\mathrm{n}}}\right), \quad (40l)$$

$$\overline{\eta}_c = 2\mathcal{C}_{\mathrm{e}}(1-t^+)\left(\overline{c}^1_{\mathrm{e,p}} - \overline{c}^1_{\mathrm{e,n}}\right), \quad (40m)$$

$$\overline{j}_{0,\mathrm{n}} = \frac{1}{L_{\mathrm{n}}}\int_0^{L_{\mathrm{n}}}\frac{\gamma_{\mathrm{n}}}{\mathcal{C}_{\mathrm{r,n}}}(c^0_{\mathrm{s,n}})^{1/2}(1-c^0_{\mathrm{s,n}})^{1/2}(1+\mathcal{C}_{\mathrm{e}}c^1_{\mathrm{e,n}})^{1/2}\,\mathrm{d}x, \quad (40n)$$

$$\overline{j}_{0,\mathrm{p}} = \frac{1}{L_{\mathrm{p}}}\int_{1-L_{\mathrm{p}}}^{1}\frac{\gamma_{\mathrm{p}}}{\mathcal{C}_{\mathrm{r,p}}}(c^0_{\mathrm{s,p}})^{1/2}(1-c^0_{\mathrm{s,p}})^{1/2}(1+\mathcal{C}_{\mathrm{e}}c^1_{\mathrm{e,p}})^{1/2}\,\mathrm{d}x, \quad (40o)$$

$$\overline{\Delta\Phi}_{\mathrm{Elec}} = -\frac{I}{\hat{\kappa}_{\mathrm{e}}\kappa_{\mathrm{e}}(1)}\left(\frac{L_{\mathrm{n}}}{3\epsilon^b_{\mathrm{n}}} + \frac{L_{\mathrm{s}}}{\epsilon^b_{\mathrm{s}}} + \frac{L_{\mathrm{p}}}{3\epsilon^b_{\mathrm{p}}}\right), \quad (40p)$$

$$\overline{\Delta\Phi}_{\mathrm{Solid}} = -\frac{I}{3}\left(\frac{L_{\mathrm{p}}}{\sigma_{\mathrm{p}}} + \frac{L_{\mathrm{n}}}{\sigma_{\mathrm{n}}}\right), \quad (40q)$$

and the overbar terms are electrode averaged quantities. The SPMe (40) consist of two independent linear PDE problems which describe the concentration of lithium in the negative and positive particles and an independent linear PDE problem which describes the concentration of lithium ions in the three regions of the electrolyte. The terminal voltage is obtained post-solution through a simple and easily interpreted algebraic expression. Since all three PDE problems are independent, the problem has a naturally parallel structure. The linearity of the PDEs is also advantageous for the application of numerical methods and the determination of simpler solutions in special cases (e.g. the SPM(S)).

5. Model comparisons

We now compare the DFN (1), SPM (20), and the SPMe (40). We take the DFN to be the 'true' voltage reading as it is the most detailed model; the validity of the DFN model itself is not a concern here. We implement the DFN model by discretising the spatial dimension using the finite volume method to convert the system of PDEs into a system of differential algebraic equations (DAEs) of index one. Before solving this system, a set of consistent initial conditions for the potentials are found numerically using Newton's method. The time evolution of the system is then performed using MATLAB's inbuilt stiff ODE and DAE solver, ODE15s. Similarly, we use the finite volume method to discretise the spatial dimensions of the SPM and SPMe and again use MATLAB's ODE15s for the time evolution. We use the same mesh to discretise the SPM, SPMe, DFN. In the x-direction, we use 30 points in the negative electrode, 20 points in the separator, and 30 points in the positive electrode. In the r-direction, we use 15 points. Numerical errors associated with the spatial discretisation, are therefore of order 10^{-2} however we hope to have limited their influence on the comparison by applying the same numerical methods to each model. As a rough comparison of computation time, the DFN model takes on the order of 5 seconds to compute one discharge whereas the SPM and SPMe take on the order of milliseconds. This significant increase in speed is vital for the study of degradation which occurs over many cycles and where parameters values are generally unknown requiring many runs of these cycles to perform parameter estimation. It should be noted that because the SPM and SPMe only produce a set of relatively unstiff ODEs upon discretisation instead of DAEs, alternative numerical solvers could be employed to further speed up the computation. However, for the purposes of comparison we choose to use the same solver as for the DFN.

We compare the three models by considering the case of a single constant-current discharge over a range of C-rates. The initial stoichiometries of the negative and positive electrode are 0.8 and 0.6, respectively, and we terminate the discharge when the terminal voltage reaches 3.2 V. For this cell a 1 C rate corresponds to a discharge current of 24 A. As provided in Table 3, we have $\mathcal{C}_{\mathrm{e}} = 5.1 \times 10^{-3}\mathcal{C}$ where $\mathcal{C}$ is the C-rate. The predicted terminal voltage of each model is presented in Figure 2.

For low C-rates, all three models match well, as expected. At higher C-rates, we observe that the SPM prediction deviates from the DFN. The SPMe shows a good improvement over the SPM, with the predictions almost indistinguishable from those of the DFN model for 0.5 C and 1 C. Unfortunately, at even higher C-rates, although the SPMe is much more accurate than the SPM, there is a discrepancy in the voltage curves near then end of the discharge. To investigate the source of this discrepancy, we have plotted the error in each components of the voltage during a 3 C discharge in Figure 3. We observe that for the majority of the

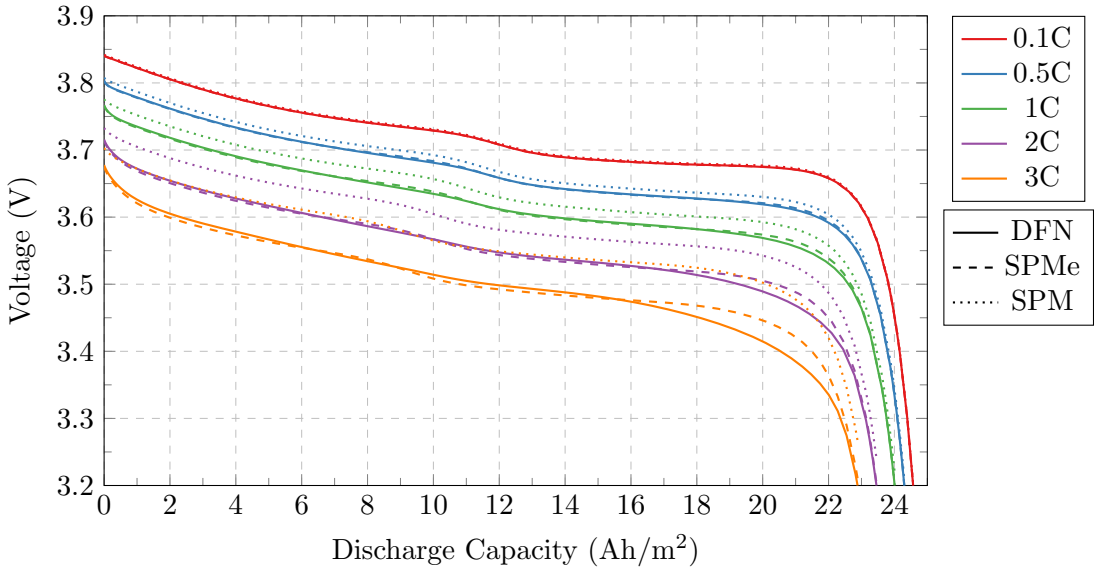

Figure 2: Constant-current discharge comparison of DFN (1), SPM (20), and SPMe (40) over a range of typical C-rates.

discharge all components of the SPMe voltage agree well with the voltage predicted by the DFN. However, near the end of the discharge, there is a large increase in the error of our solution as was observed in Figure 2. Around 60-70% of this error is due to a poor estimation of the electrode-averaged OCV. This error occurs when the OCV becomes very nonlinear. If we extend our asymptotic expansion of the open circuit voltage, $U_{\mathrm{k}}(c_{\mathrm{k}})$ to to second order, we obtain the term $\mathcal{C}_{\mathrm{e}}^2 U_{\mathrm{k}}''(c_{\mathrm{s,k}}^0)(c_{\mathrm{s,k}}^1)^2/2$. When the OCV is very nonlinear, $U_{\mathrm{k}}''(c_{\mathrm{s,k}}^0)$ becomes large. To account for this we can consider the distinguished limit in which

$$U_{\mathrm{k}}''(c_{\mathrm{s,k}}^0) \sim \mathcal{O}(\mathcal{C}_{\mathrm{e}}^{-1}). \tag{41}$$

In this limit, we cannot avoid solving for the concentrations in all the particles in each electrode and therefore lose a large portion of the computational simplicity of the SPM and SPMe. We have developed and implemented a numerical scheme for this limit and found that it does indeed correct the voltage discrepancy. However, because of the increased computational complexity but we do not discuss it in detail within this paper.

To further confirm the accuracy of the SPMe, we compare the internal states predicted by the SPMe and DFN. These are presented for a 1 C constant current discharge in Figure 4. We observe good agreement between the two sets of model predictions. However, two key discrepancies may be observed: the first in the negative electrode stoichiometry and the second in the electrolyte concentration at late times. We note that the apparent discrepancy in the negative electrode potential is only due to the scale employed in Figure 4 and is $\mathcal{O}(\mathcal{C}_{\mathrm{e}}^2)$.

The discrepancy in the negative electrode stoichiometry is a result of the SPMe using only the leading-order equations in $\mathcal{C}_{\mathrm{e}}$ within the electrode particles, which is the electrode averaged concentration in the particles. This is the same approximation as employed by the SPM and is therefore only accurate to $\mathcal{O}(\mathcal{C}_{\mathrm{e}})$. It is possible to additionally solve for the first-

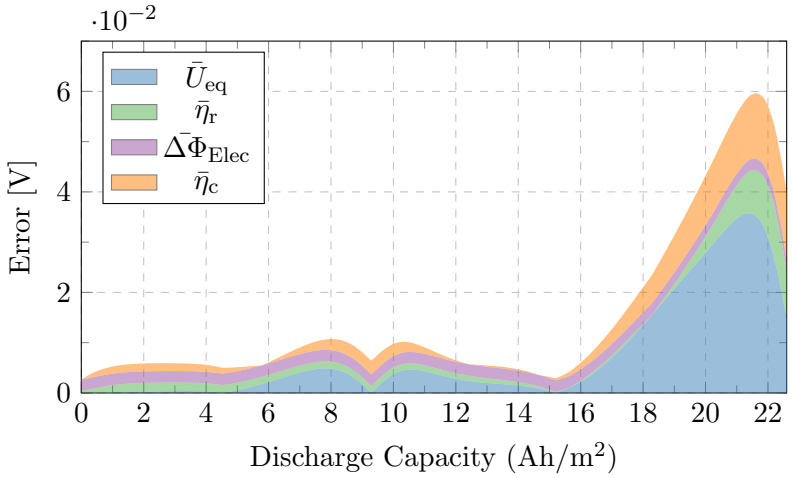

Figure 3: Overpotential errors between the SPMe and DFN.

order correction in the particles, however, this requires solving a diffusion equation on each particle instead of just one for the electrode-average particle. This increases the computational complexity of the model so we have omitted it here.

The discrepancy in the electrolyte concentration at late time is fundamentally connected to the discrepancy in the voltage curves we observed in Figure 2. As we already discussed, this is caused by the OCV being nonlinear and the term $U_{\text{k}}''(c_{\text{s,k}}^0)$ becoming large. We must then consider the distiguished limit in which (41) holds. In this limit, there is a more heterogeneous interfacial current density and so the electrode-averaged current density source/sink terms in (40b) and (40c) are replaced by heterogeneous versions. We have implemented a numerical scheme for this limit and can confirm that this discrepancy is accounted for in this way. However, as already stated, this limit requires one to solve for the concentration in all the particles and is therefore much more computationally expensive than the models of concern in this paper.

6. Critical assessment of variations on the SPMe in the literature

6.1. Overview of models

There are a number of alternative models in the literature that extend the SPM in an ad-hoc manner to account for electrolyte effects [14, 15, 16, 17, 18, 19]. In this section, we highlight the key differences between these other models and the canonical SPMe (40) presented here. We have chosen to compare a subset of the models which cover the variety of ad-hoc models available. To do this, we have converted the models to dimensionless form using the scalings in (2). In some papers the model is discretised during development. We view the choice of discretisation to be a numerical method instead of a feature of the model itself. Therefore, we have converted each model into continuum form to highlight differences in the underlying models. We do not aim here to study the benefits and drawbacks of different numerical methods.

A common theme in the models from the literature is to replace the electrode-averaged concentration overpotential and electrode-averaged electrolyte ohmic losses with pointwise

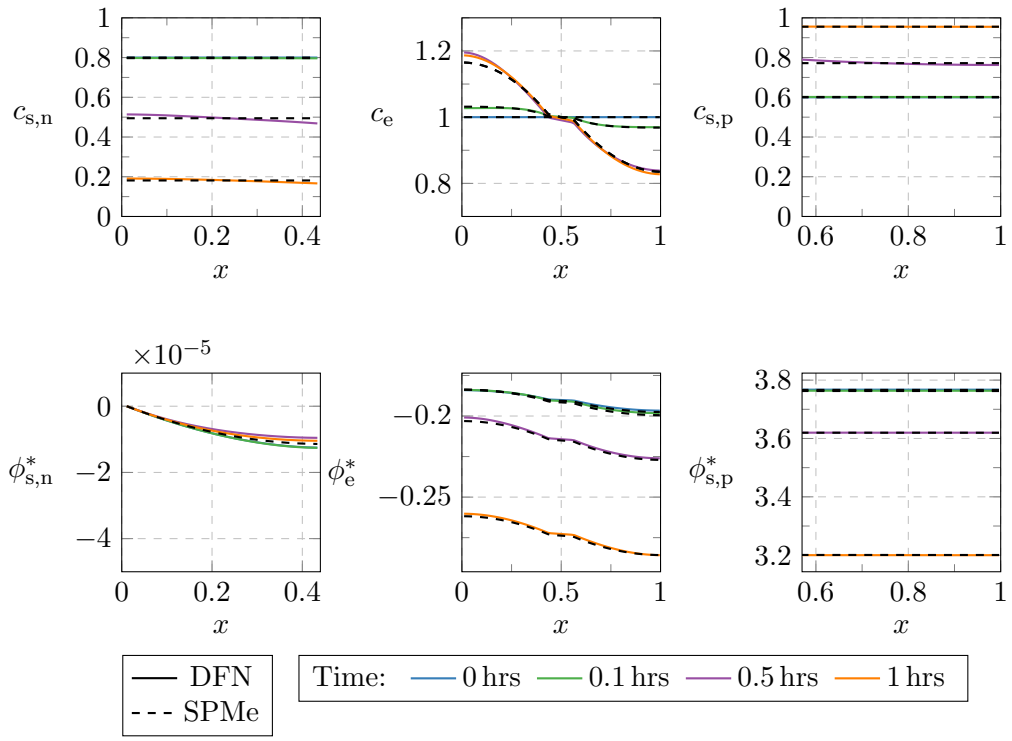

Figure 4: Comparison of DFN and SPMe internal states during a 1 C constant current discharge. The DFN solution is given by the solid lines and the SPMe solution by the closest black dashed line. Note that some of the black dashed lines lie upon others so it appears that there are fewer black dashed lines than solid lines.

versions. It is also common to neglect the solid phase ohmic losses (this is a reasonable assumption since we have already observed these to be small). The general form of the terminal voltage expression used in the literature is then:

$$V = \overline{U}_{\text{eq}} + \overline{\eta}_{\text{r}} + \eta_{\text{c}}\big|_{x_{\text{n}}=0,x_{\text{p}}=1} + \Delta\Phi_{\text{Elec}}\big|_{x_{\text{n}}=0,x_{\text{p}}=1}. \tag{42}$$

The involves mixing the electrode-averaged and pointwise terms and therefore accuracy of $\mathcal{O}(\mathcal{C}_{\text{e}}^2)$ cannot be ensured.

We begin by considering the model proposed by Perez et. al. in [15]. Firstly, the electrolyte flux (40c) is replaced by the expression (after converting to our notation)

$$N^1_{\text{e,k}} = -\epsilon^b_{\text{k}} D_{\text{e}}(1 + \mathcal{C}_{\text{e}} c^1_{\text{e,k}}) \frac{\partial c^1_{\text{e,k}}}{\partial x} + \begin{cases} \frac{x t^+ I}{\gamma_{\text{e}} L_{\text{n}}}, & \text{k} = \text{n}, \\ \frac{t^+ I}{\gamma_{\text{e}}}, & \text{k} = \text{s} \\ \frac{(1-x) t^+ I}{\gamma_{\text{e}} L_{\text{p}}}, & \text{k} = \text{p}, \end{cases} \quad \text{for k} \in \{\text{n, s, p}\}. \tag{43}$$

Due to the the presence of the nonlinear diffusion coefficient the electrolyte problem is nonlinear, while that for the SPMe, (40), is linear. Since the other terms are unchanged, this nonlinear form is also accurate up to $\mathcal{O}(\mathcal{C}_{\text{e}}^2)$. This nonlinear form introduces some (but not all) higher order terms, which in practice may increase accuracy but this cannot be ensured (there is also a chance it could reduce accuracy). Secondly, the electrode-averaged concentration overpotential (40m) and the electrode-averaged electrolyte Ohmic losses (40p) are

replaced by their pointwise versions:

$$\eta_{\mathrm{c}}\big|_{x_{\mathrm{n}}=0,x_{\mathrm{p}}=1} = 2(1-t^{+})\log\left(\frac{1+\mathcal{C}_{\mathrm{e}}c^{1}_{\mathrm{e,p}}\big|_{x=1}}{1+\mathcal{C}_{\mathrm{e}}c^{1}_{\mathrm{e,p}}\big|_{x=0}}\right), \tag{44}$$

$$\Delta\Phi_{\mathrm{Elec}}\big|_{x_{\mathrm{n}}=0,x_{\mathrm{p}}=1} = -\frac{I}{2\hat{\kappa}_{\mathrm{e}}\overline{\kappa}^{\mathrm{eff}}_{\mathrm{e}}}\left(L_{\mathrm{n}}+2L_{\mathrm{s}}+L_{\mathrm{p}}\right), \tag{45}$$

respectively (note that to get (45) we have corrected the sign of the expression in [15]). Here $\overline{\kappa}^{\mathrm{eff}}_{\mathrm{e}}$ is the dimensionless effective conductivity averaged across the entire cell, with the effective conductivity defined by $\kappa^{\mathrm{eff}}_{\mathrm{e}}(c_{\mathrm{e,k}}) = \epsilon^{b}_{\mathrm{k}}\kappa_{\mathrm{e}}(c_{\mathrm{e,k}})$. The terminal voltage is then given by (42). Additionally, (45) requires that $\kappa^{\mathrm{eff}}_{e}(c_{\mathrm{e,k}}) \approx \overline{\kappa}^{\mathrm{eff}}_{e}$ throughout the cell. With this assumption, $\mathcal{O}(\mathcal{C}^{2}_{\mathrm{e}})$ accuracy cannot be ensured for all values of ϵ_{n}, ϵ_{s}, and ϵ_{p}. Finally, solid phase Ohmic losses are neglected and Ohmic losses due to the presence of SEI are included; we shall neglect the SEI terms in our comparisons noting that (40) can be easily extended to include them.

The model presented by Prada et. al. [16] also employs (44) for the concentration overpotential. However, the electrolyte Ohmic losses are taken to be

$$\Delta\Phi_{\mathrm{Elec}}\big|_{x_{\mathrm{n}}=0,x_{\mathrm{p}}=1} = -\frac{I}{2\hat{\kappa}_{\mathrm{e}}}\left(\frac{L_{\mathrm{n}}}{\epsilon^{b}_{\mathrm{n}}\overline{\kappa}_{\mathrm{e,n}}}+2\frac{L_{s}}{\epsilon^{b}_{\mathrm{s}}\overline{\kappa}_{\mathrm{e,s}}}+\frac{L_{\mathrm{p}}}{\epsilon^{b}_{\mathrm{p}}\overline{\kappa}_{\mathrm{e,p}}}\right), \tag{46}$$

where

$$\begin{aligned}
\overline{\kappa}_{\mathrm{e,n}} &= \int_{0}^{L_{\mathrm{n}}} \kappa_{\mathrm{e}}\left(1+\mathcal{C}_{\mathrm{e}}c^{1}_{\mathrm{e,n}}\right)\,\mathrm{d}x,\\
\overline{\kappa}_{\mathrm{e,s}} &= \int_{L_{\mathrm{n}}}^{1-L_{\mathrm{p}}} \kappa_{\mathrm{e}}\left(1+\mathcal{C}_{\mathrm{e}}c^{1}_{\mathrm{e,s}}\right)\,\mathrm{d}x,\\
\overline{\kappa}_{e,p} &= \int_{1-L_{\mathrm{p}}}^{1} \kappa_{\mathrm{e}}\left(1+\mathcal{C}_{\mathrm{e}}c^{1}_{\mathrm{e,p}}\right)\,\mathrm{d}x.
\end{aligned} \tag{47}$$

Whilst (46) does not rely upon the assumption that $\kappa^{\mathrm{eff}}_{\mathrm{e}}(c_{\mathrm{e,k}}) \approx \overline{\kappa}^{\mathrm{eff}}_{\mathrm{e}}$, its form is still a result of considering the pointwise electrolyte potential difference instead of the electrode averaged difference. In addition to these differences, Prada et. al. [16] take the exchange current densities: $\overline{j}_{0,\mathrm{n}}$ and $\overline{j}_{0,\mathrm{p}}$ to be constant. In terms of accurately reproducing DFN results, this simplification has a clear disadvantage as the reaction overpotentials are strong functions of the lithium and lithium ion concentrations.

The model developed by Han et. al [17] is the same as that presented by Prada et. al. [16] without the additional assumption of constant exchange current densities. That is, Han et. al. [17] employ (44) and (46), which are the current collector to current collector concentration overpotential, and electrolyte ohmic losses, respectively. Han et. al. [17] note the tendency for their model to over-correct the voltage when accounting for electrolyte effects. We suspect the use of pointwise terms is the cause.

The model presented by Kemper et. al. [14] is quite different to the others we have discussed. Firstly, the model is presented as a set of ODEs instead of PDEs. These ODEs are derived by spatially discretising the underlying PDEs. Whilst this particular discretisation may be useful, we consider this to be a numerical method and not a feature of the model itself. Since we aim to compare the underlying simplified models directly, we have converted these ODEs back into PDEs. It turns out that these PDEs, which describe the concentrations in

the electrode particles and the electrolyte, are the same as those used in our model. However, the expression for the terminal voltage is very different and it is not easy to prescribe meaning to each of the individual components; we have however attempted this. We have converted the voltage from [14] into dimensionless form and provided details in Appendix C to be clear about the exact model we are comparing. It was unclear if the components of the voltage correspond to electrode-averaged or pointwise quantities so we have left this unstated.

6.2. Model comparison

We compare the variations of the SPMe in the literature and our canonical SPMe. To do this, we consider a range of constant current discharge rates and then compare the error of each model in predicting the DFN terminal voltage. Our results are presented in Figure 5, where we compare the models in [15, 17, 14]. Each of these models is of comparable complexity so we do not compare solution times, which are very similar. We observe that across all discharge rates, our canonical SPMe outperforms the other models from the literature. In particular, our canonical SPMe is consistently an order of magnitude more accurate than the models in Perez et. al. [15] and Kemper et. al [14]. Furthermore, at higher C-rates, the errors in the models from the literature approach being of the order of 1 V whereas our SPMe produces errors which never exceed the order of 0.1 V. Additionally, as we would expect, our model converges to the DFN solution at a faster rate than the other models, with the model in Han et. al. diverging as the C-rate tends to zero. We attribute the main gains of our model to the consistent electrode-averaged OCPs, overpotentials, and Ohmic losses in our terminal voltage expression.

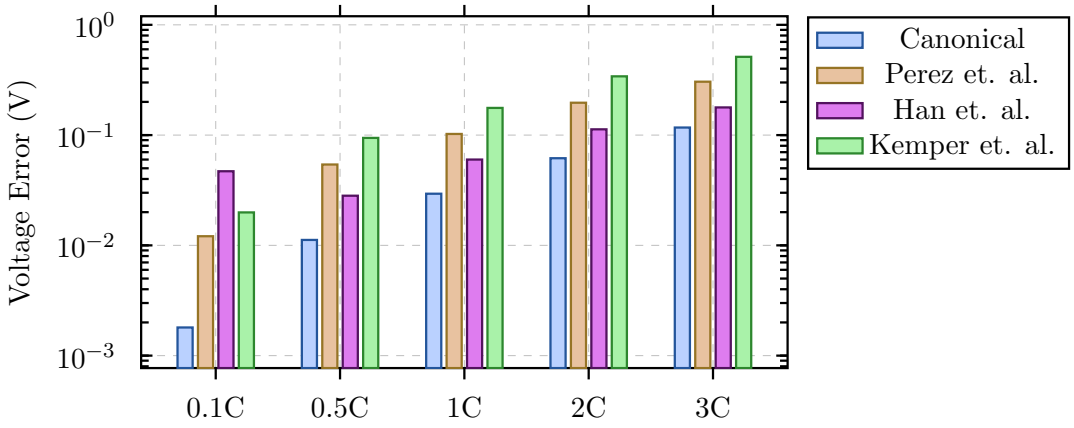

Figure 5: Comparison of versions of the SPMe: Canonical (40), Perez et. al. [15], Han et. al. [17], and Kemper et. al. [14]. The models are compared by considering the ℓ^2-error of the simplified model voltage prediction vs the DFN (1) voltage prediction.

7. Dimensional model summary and conditions for application

We now present a summary of the dimensional SPMe alongside the conditions which should be met before applying the model. The purpose of this section is to serve as a reference, which is easily accessible to those not interested in the full details of the model derivation. For the purpose of this section, we will drop the superscript notation, which was used to indicated the

asymptotic order of a variable. Also, to be consistent with the rest of the paper, we employ a superscript $*$ to denote dimensional quanitites. By reapplying our scalings in (2) to (40) and combining the leading-order and first-order equations for the electrolyte concentration, we obtain

Governing Equations

$$\frac{\partial c^*_{\mathrm{s,k}}}{\partial t^*} = \frac{1}{(r^*)^2}\frac{\partial}{\partial r^*}\left((r^*)^2 D^*_{\mathrm{s,k}}(c^*_{\mathrm{s,k}})\frac{\partial c^*_{\mathrm{s,k}}}{\partial r^*}\right), \quad \mathrm{k} \in \{\mathrm{n},\, \mathrm{p}\}, \tag{48a}$$

$$\epsilon_{\mathrm{k}}\frac{\partial c^*_{\mathrm{e,k}}}{\partial t^*} = -\frac{\partial N^*_{\mathrm{e,k}}}{\partial x^*} + \begin{cases} \frac{I^*}{F^* L^*_{\mathrm{n}}}, & \mathrm{k} = \mathrm{n} \\ 0, & \mathrm{k} = \mathrm{s} \\ -\frac{I^*}{F^* L^*_{\mathrm{p}}}, & \mathrm{k} = \mathrm{p} \end{cases} \quad \mathrm{k} \in \{\mathrm{n},\, \mathrm{s},\, \mathrm{p}\}, \tag{48b}$$

$$N^*_{\mathrm{e,k}} = -\epsilon^{\mathrm{b}}_{\mathrm{k}} D^*_{\mathrm{e}}(c^*_{\mathrm{e,typ}})\frac{\partial c^*_{\mathrm{e,k}}}{\partial x} + \begin{cases} \frac{x^* t^+ I^*}{F^* L^*_{\mathrm{n}}}, & \mathrm{k} = \mathrm{n} \\ \frac{t^+ I^*}{F^*}, & \mathrm{k} = \mathrm{s} \\ \frac{(L^* - x^*) t^+ I^*}{F^* L_{\mathrm{p}}}, & \mathrm{k} = \mathrm{p} \end{cases} \quad \mathrm{k} \in \{\mathrm{n},\, \mathrm{s},\, \mathrm{p}\}, \tag{48c}$$

Boundary Conditions

$$\left.\frac{\partial c^*_{\mathrm{s,k}}}{\partial r^*}\right|_{r^*=0} = 0, \quad \left. -D^*_{\mathrm{s,k}}(c^*_{\mathrm{s,k}})\frac{\partial c^*_{\mathrm{s,k}}}{\partial r^*}\right|_{r^*=R^*_{\mathrm{k}}} = \begin{cases} \frac{I^*}{F^* a^*_{\mathrm{n}} L^*_{\mathrm{n}}} & \mathrm{k} = \mathrm{n} \\ -\frac{I^*}{F^* a^*_{\mathrm{p}} L^*_{\mathrm{p}}} & \mathrm{k} = \mathrm{p} \end{cases} \quad \mathrm{k} \in \{\mathrm{n},\, \mathrm{p}\}, \tag{48d}$$

$$N^*_{\mathrm{e,n}}\big|_{x^*=0} = 0, \quad N^*_{\mathrm{e,p}}\big|_{x^*=L^*} = 0, \tag{48e}$$

$$c^*_{\mathrm{e,n}}|_{x^*=L^*_{\mathrm{n}}} = c^*_{\mathrm{e,s}}|_{x^*=L^*_{\mathrm{n}}}, \quad N^*_{\mathrm{e,n}}\big|_{x^*=L^*_{\mathrm{n}}} = N^*_{\mathrm{e,s}}\big|_{x^*=L^*_{\mathrm{n}}}, \tag{48f}$$

$$c^*_{\mathrm{e,s}}|_{x^*=L^*-L^*_{\mathrm{p}}} = c^*_{\mathrm{e,p}}|_{x^*=L^*-L^*_{\mathrm{p}}}, \quad N^*_{\mathrm{e,s}}\big|_{x^*=L^*-L^*_{\mathrm{p}}} = N^*_{\mathrm{e,p}}\big|_{x^*=L^*-L^*_{\mathrm{p}}}. \tag{48g}$$

Initial Conditions

$$c^*_{\mathrm{s,k}}(r^*, 0) = c^*_{\mathrm{k},0}, \quad \mathrm{k} \in \{\mathrm{n},\, \mathrm{p}\}, \tag{48h}$$

$$c^*_{\mathrm{e,k}}(x^*, 0) = c^*_{\mathrm{e,typ}}, \quad \mathrm{k} \in \{\mathrm{n},\, \mathrm{s},\, \mathrm{p}\}, \tag{48i}$$

Terminal Voltage

$$V^* = \overline{U}^*_{\mathrm{eq}} + \overline{\eta}^*_r + \overline{\eta}^*_c + \overline{\Delta\Phi}^*_{\mathrm{Elec}} + \overline{\Delta\Phi}^*_{\mathrm{Solid}}, \tag{48j}$$

where

$$\overline{U}^*_{\mathrm{eq}} = U^*_{\mathrm{p}}\left(c^*_{\mathrm{s,p}}\big|_{r^*=R^*_{\mathrm{p}}}\right) - U^*_{\mathrm{n}}\left(c^*_{\mathrm{s,n}}\big|_{r^*=R^*_{\mathrm{n}}}\right), \tag{48k}$$

$$\overline{\eta}^*_r = -\frac{2R^*T^*}{F^*}\sinh^{-1}\left(\frac{I^*}{a^*_{\mathrm{p}}\overline{j}^*_{0,\mathrm{p}}L^*_{\mathrm{p}}}\right) - \frac{2R^*T^*}{F^*}\sinh^{-1}\left(\frac{I^*}{a^*_{\mathrm{n}}\overline{j}^*_{0,\mathrm{n}}L^*_{\mathrm{n}}}\right), \tag{48l}$$

$$\overline{\eta}^*_c = \frac{2R^*T^*}{F^*c^*_{\mathrm{e,typ}}}(1-t^+)\left(\overline{c}^*_{\mathrm{e,p}} - \overline{c}^*_{\mathrm{e,n}}\right), \tag{48m}$$

$$\overline{j}^*_{0,\mathrm{n}} = \frac{1}{L^*_{\mathrm{n}}}\int_0^{L^*_{\mathrm{n}}} m^*_{\mathrm{n}}(c^*_{\mathrm{s,n}})^{1/2}(c^*_{\mathrm{s,n,max}} - c^*_{\mathrm{s,n}})^{1/2}(c^*_{\mathrm{e,n}})^{1/2}\,\mathrm{d}x^*, \tag{48n}$$

$$\overline{j}^*_{0,\mathrm{p}} = \frac{1}{L^*_{\mathrm{p}}}\int_{L^*-L^*_{\mathrm{p}}}^{L^*} m^*_{\mathrm{p}}(c^*_{\mathrm{s,p}})^{1/2}(c^*_{\mathrm{s,p,max}} - c^*_{\mathrm{s,p}})^{1/2}(c^*_{\mathrm{e,p}})^{1/2}\,\mathrm{d}x^*, \tag{48o}$$

$$\overline{\Delta\Phi}^*_{\mathrm{Elec}} = -\frac{I^*}{\kappa^*_{\mathrm{e}}(c^*_{\mathrm{e,typ}})}\left(\frac{L^*_{\mathrm{n}}}{3\epsilon^b_{\mathrm{n}}} + \frac{L^*_{\mathrm{s}}}{\epsilon^b_{\mathrm{s}}} + \frac{L^*_{\mathrm{p}}}{3\epsilon^b_{\mathrm{p}}}\right), \tag{48p}$$

$$\overline{\Delta\Phi}^*_{\mathrm{Solid}} = -\frac{I^*}{3}\left(\frac{L^*_{\mathrm{p}}}{\sigma^*_{\mathrm{p}}} + \frac{L^*_{\mathrm{n}}}{\sigma^*_{\mathrm{n}}}\right). \tag{48q}$$

We have provided the conditions that ensure the validity of (48) in Table 4.

Parameter combination	Required size	Interpretation
$\mathcal{C}_{\mathrm{e}} = I^*_{\mathrm{typ}}L^*/(D^*_{\mathrm{e,typ}}F^*c^*_{\mathrm{n,max}})$	$\ll 1$	Fast lithium ion diffusion in electrolyte
$R^*T^*\sigma^*_{\mathrm{k}}/(F^*I^*_{\mathrm{typ}}L^*)$	$\gg 1$	Large solid conductivity
$R^*T^*\kappa^*_{\mathrm{e,typ}}/(F^*I^*_{\mathrm{typ}}L^*)$	$\gg 1$	Large electrolyte conductivity
$(R^*_{\mathrm{k}})^2 I^*_{\mathrm{typ}}/(D^*_{\mathrm{s,k}}F^*c^*_{\mathrm{n,max}}L^*)$	$\ll 1/\mathcal{C}_{\mathrm{e}}$	Solid diffusion occurs on a shorter or similar timescale to a discharge
$I^*_{\mathrm{typ}}/(m^*_{\mathrm{k}}a^*_{\mathrm{k}}(c^*_{\mathrm{e,typ}})^{1/2}c^*_{\mathrm{n,max}}L^*)$	$\ll 1/\mathcal{C}_{\mathrm{e}}$	Reactions occur on a shorter or similar timescale to a discharge

Table 4: The key conditions to be satisfied for the application of (48). In addition, it is required that $\mathcal{C}_{\mathrm{e}} \ll L^*_{\mathrm{k}}/L^* \ll 1/\mathcal{C}_{\mathrm{e}}$, $\mathcal{C}_{\mathrm{e}} \ll c_{\mathrm{p,max}}/c_{\mathrm{n,max}} \ll 1/\mathcal{C}_{\mathrm{e}}$, and $\mathcal{C}_{\mathrm{e}} \ll c_{\mathrm{e,typ}}/c_{\mathrm{n,max}} \ll 1/\mathcal{C}_{\mathrm{e}}$, which are true in practical situations.

If the conditions in Table 4 are met then the model error at a particular time is of size

$$\max\left(\left(\frac{I^*_{\mathrm{typ}}L^*}{D^*_{\mathrm{e,typ}}F^*c^*_{\mathrm{n,max}}}\right)^2, \left(\frac{I^*_{\mathrm{typ}}L^*}{D^*_{\mathrm{e,typ}}}\right)^2\left(\frac{1}{F^*R^*T^*}\right)(U^*_{\mathrm{k}})''\right) \tag{49}$$

where the term $(U^*_{\mathrm{k}})''$ is the second derivative of the open circuit potential in electrode k, which accounts for the decrease in accuracy when the open circuit potential is significantly nonlinear. In situations where transient effects are not important (e.g. when the current varies on timescales longer than the electrolyte diffusion timescale), the same degree of accuracy can be achieved by employing the dimensional equivalent to the the SPMe(S); this is done by neglecting the time derivative term in the electrolyte equation (48b).

8. Summary and further work

We have systematically derived simplified mathematical models from the standard DFN model through the use of asymptotic methods. The leading-order model we derive, (20), is commonly used in the control community. By considering higher-order effects, we have extended this model to develop a canonical SPMe which is applicable over a larger range of operating conditions. The canonical SPMe has been shown to give good agreement with the DFN and to perform better than all other reduced models available in the literature. A key result of this paper is to identify the requirement of writing the output voltage expression in terms of the electrode-averaged OCV, overpotentials, and Ohmic losses a step which was overlooked in previous literature. Finally, our systematic approach has allowed us to identify the reasons for discrepancies in the predictions of the SPMe and identify the minimal extensions required for them to be corrected.

There are a number of possible additional physical mechanisms that are of interest to incorporate into a battery model. These include mechanical effects, thermal effects, and degradation mechanisms. One approach would be to simply introduce these effects in an ad-hoc manner to existing simple models without consideration of their interactions within the context of a more complicated model such as the DFN. The systemic approach employed in this paper may also be used to derive reduced models with additional physics whilst still retaining the most important effects.

Appendix A. Electrode-averaged quantities

$$\overline{c}^1_{\mathrm{e,n}} = \frac{(1-t^+)I}{6\gamma_{\mathrm{e}}D_{\mathrm{e}}(1)}\left(2\left(\frac{L_{\mathrm{p}}^2}{\epsilon_{\mathrm{p}}^b}-\frac{L_{\mathrm{n}}^2}{\epsilon_{\mathrm{n}}^b}\right)+\frac{2L_{\mathrm{n}}}{\epsilon_{\mathrm{n}}^b}+\frac{3L_{\mathrm{s}}}{\epsilon_{\mathrm{s}}^b}(L_{\mathrm{p}}-L_{\mathrm{n}}+1)\right) \tag{A.1}$$

$$\overline{c}^1_{\mathrm{e,p}} = \frac{(1-t^+)I}{6\gamma_{\mathrm{e}}D_{\mathrm{e}}(1)}\left(2\left(\frac{L_{\mathrm{p}}^2}{\epsilon_{\mathrm{p}}^b}-\frac{L_{\mathrm{n}}^2}{\epsilon_{\mathrm{n}}^b}\right)-\frac{2L_{\mathrm{p}}}{\epsilon_{\mathrm{p}}^b}+\frac{3L_{\mathrm{s}}}{\epsilon_{\mathrm{s}}^b}(L_{\mathrm{p}}-L_{\mathrm{n}}-1)\right) \tag{A.2}$$

$$\overline{\phi}^1_{\mathrm{e,n}} = \tilde{\phi}_{\mathrm{e}} + 2(1-t^+)\overline{c}^1_{\mathrm{e,n}} + \frac{IL_{\mathrm{n}}}{\hat{\kappa}'_{\mathrm{e}}\kappa_{\mathrm{e}}(1)}\left(\frac{1}{3\epsilon_{\mathrm{n}}^b}-\frac{1}{\epsilon_{\mathrm{s}}^b}\right) \tag{A.3}$$

$$\overline{\phi}^1_{\mathrm{e,p}} = \tilde{\phi}_{\mathrm{e}} + 2(1-t^+)\overline{c}^1_{\mathrm{e,p}} + \frac{IL_{\mathrm{p}}}{\hat{\kappa}'_{\mathrm{e}}\kappa_{\mathrm{e}}(1)}\left(\frac{1}{\epsilon_{\mathrm{s}}^b}-\frac{1}{3\epsilon_{\mathrm{p}}^b}\right)-\frac{I}{\hat{\kappa}'_{\mathrm{e}}\kappa_{\mathrm{e}}(1)\epsilon_{\mathrm{s}}^b} \tag{A.4}$$

$$\overline{\phi}^1_{\mathrm{s,n}} = -\frac{IL_{\mathrm{n}}}{3\sigma'_{\mathrm{n}}} \tag{A.5}$$

$$\overline{\varphi}^1_{\mathrm{s,p}} = \frac{IL_{\mathrm{p}}}{3\sigma'_{\mathrm{p}}} \tag{A.6}$$

$$\overline{\phi}^1_{\mathrm{s,p}} = \overline{\varphi}_{\mathrm{s,p}} + V^1 \tag{A.7}$$

Appendix B. Electrolyte constants of integration

$$\phi_{\mathrm{e}}^0 = -U_{\mathrm{n}}(c_{\mathrm{s,n}}^0\big|_{r_{\mathrm{n}}=1}) - \eta_{\mathrm{n}}^0 \tag{B.1}$$

$$\tilde{\phi}_{\mathrm{e}} = -2(1+t^+)\overline{c}^1_{\mathrm{e,n}} + \frac{IL_{\mathrm{n}}}{\gamma_{\mathrm{e}}\kappa_{\mathrm{e}}(1)}\left(\frac{1}{3\epsilon_{\mathrm{n}}^b}-\frac{1}{\epsilon_{\mathrm{s}}^b}\right) + \overline{\phi}^1_{\mathrm{s,n}} - \overline{\eta}^1_{\mathrm{n}} \tag{B.2}$$

Appendix C. Dimenionless voltage from [14]

Although the form of the voltage in [14] is not given explicitly, we assume that it is given by $\phi_s(0^+,t)-\phi_s(0^-,t)$ (in their notation), which is the potential difference between the solid phase potential evaluated at the positive and negative current collectors. We also note that in [14] current has been defined in the direction of flow of positive charge (opposite of the convention used here) so we account for the sign change here. The model in [14] is then taken to be:

$$V = U_{\text{eq}} + \eta_{\text{r}} + \eta_{\text{c}} + \Delta\Phi_{\text{Elec}}, \tag{C.1}$$

$$U_{\text{eq}} = U_{\text{p}}(c^0_{\text{s,p}}\big|_{r=1}) - U_{\text{n}}(c^0_{\text{s,n}}\big|_{r=1}), \tag{C.2}$$

$$\begin{aligned}\eta_{\text{r}} =& -2\sinh^{-1}\left(\frac{I}{L_{\text{p}}j_{0,\text{p}}(1)}\right) - 2\sinh^{-1}\left(\frac{I}{L_{\text{n}}j_{0,\text{n}}(0)}\right)\\ &+\frac{2\mathcal{C}_{\text{e}}}{\gamma_{\text{e}}}\frac{\sigma_{\text{p}}}{\overline{\kappa}_{\text{e,p}}+\frac{\mathcal{C}_{\text{e}}}{\gamma_{\text{e}}}\sigma_{\text{p}}}\left(\sinh^{-1}\left(\frac{I}{L_{\text{p}}j_{0,\text{p}}(1)}\right)-\sinh^{-1}\left(\frac{I}{L_{\text{p}}j_{0,\text{p}}(1-L_{\text{p}})}\right)\right)\\ &+\frac{2\mathcal{C}_{\text{e}}}{\gamma_{\text{e}}}\frac{\sigma_{\text{n}}}{\overline{\kappa}_{\text{e,n}}+\frac{\mathcal{C}_{\text{e}}}{\gamma_{\text{e}}}\sigma_{\text{n}}}\left(\sinh^{-1}\left(\frac{I}{L_{\text{n}}j_{0,\text{n}}(0)}\right)-\sinh^{-1}\left(\frac{I}{L_{\text{n}}j_{0,\text{n}}(L_{\text{n}})}\right)\right),\end{aligned} \tag{C.3}$$

$$\begin{aligned}\eta_c =& 2(1-t^+)\left(\frac{\overline{\kappa}_{\text{e,p}}}{\overline{\kappa}_{\text{e,p}}+\frac{\mathcal{C}_{\text{e}}}{\gamma_{\text{e}}}\sigma_{\text{p}}}\log\left(\frac{1+\mathcal{C}_{\text{e}}c^1_{\text{e,p}}\big|_{x=1}}{1+\mathcal{C}_{\text{e}}c^1_{\text{e,p}}\big|_{x=1-L_{\text{p}}}}\right)+\log\left(\frac{1+\mathcal{C}_{\text{e}}c^1_{\text{e,s}}\big|_{x=L_{\text{n}}}}{1+\mathcal{C}_{\text{e}}c^1_{\text{e,s}}\big|_{x=1-L_{\text{p}}}}\right)\right.\\ &\left.+\frac{\overline{\kappa}_{\text{e,n}}}{\overline{\kappa}_{\text{e,n}}+\frac{\mathcal{C}_{\text{e}}}{\gamma_{\text{e}}}\sigma_{\text{n}}}\log\left(\frac{1+\mathcal{C}_{\text{e}}c^1_{\text{e,n}}\big|_{x=L_{\text{n}}}}{1+\mathcal{C}_{\text{e}}c^1_{\text{e,n}}\big|_{x=0}}\right)\right),\end{aligned} \tag{C.4}$$

$$\Delta\Phi_{\text{Elec}} = -\frac{I}{\hat{\kappa}_{\text{e}}}\left(\frac{L_{\text{n}}}{\overline{\kappa}_{\text{e,n}}+\mathcal{C}_{\text{e}}\gamma_{\text{e}}\sigma_n}-\frac{L_s}{\overline{\kappa}_{\text{e,s}}}+\frac{L_{\text{p}}}{\overline{\kappa}_{\text{e,p}}+\mathcal{C}_{\text{e}}\gamma_{\text{e}}\sigma_p}\right) \tag{C.5}$$

where $\overline{\kappa}_{\text{e,k}}$ is given by (47) and

$$j_{0,\text{k}} = \frac{\gamma_{\text{k}}}{\mathcal{C}_{\text{r,k}}}(c^0_{\text{s,k}})^{1/2}(1-c^0_{\text{s,k}})^{1/2}(1+\mathcal{C}_{\text{e}}c^1_{\text{e,k}})^{1/2}.$$

References

[1] M. Doyle, T. F. Fuller, J. Newman, Modeling of galvanostatic charge and discharge of the lithium/polymer/insertion cell, Journal of the Electrochemical Society 140 (6) (1993) 1526–1533.

[2] T. F. Fuller, Simulation and Optimization of the Dual Lithium Ion Insertion Cell, Journal of The Electrochemical Society 141 (1) (1994) 1. doi:10.1149/1.2054684.
URL http://jes.ecsdl.org/cgi/doi/10.1149/1.2054684

[3] J. Newman, K. E. Thomas-Alyea, Electrochemical systems, John Wiley & Sons, 2012.

[4] A. M. Bizeray, S. Zhao, S. R. Duncan, D. A. Howey, Lithium-ion battery thermal-electrochemical model-based state estimation using orthogonal collocation and a modified extended Kalman filter, Journal of Power Sources 296 (2015) 400–412. arXiv:1506.08689, doi:10.1016/j.jpowsour.2015.07.019.

[5] L. Cai, R. E. White, Lithium ion cell modeling using orthogonal collocation on finite elements, Journal of Power Sources 217 (2012) 248–255. doi:10.1016/j.jpowsour.2012.06.043.
URL http://linkinghub.elsevier.com/retrieve/pii/S0378775312010439

[6] Y. Zeng, P. Albertus, R. Klein, N. Chaturvedi, A. Kojic, M. Z. Bazant, J. Christensen, Efficient conservative numerical schemes for 1d nonlinear spherical diffusion equations with applications in battery modeling, Journal of The Electrochemical Society 160 (9) (2013) A1565–A1571.

[7] R. N. Methekar, V. Ramadesigan, J. C. Pirkle, V. R. Subramanian, A perturbation approach for consistent initialization of index-1 explicit differential-algebraic equations arising from battery model simulations, Computers and Chemical Engineering 35 (11) (2011) 2227–2234. doi:10.1016/j.compchemeng.2011.01.003.

[8] V. R. Subramanian, V. Boovaragavan, V. Ramadesigan, M. Arabandi, Mathematical Model Reformulation for Lithium-Ion Battery Simulations: Galvanostatic Boundary Conditions, Journal of The Electrochemical Society 156 (4) (2009) A260. doi:10.1149/1.3065083.
URL http://jes.ecsdl.org/cgi/doi/10.1149/1.3065083

[9] P. W. C. Northrop, V. Ramadesigan, S. De, V. R. Subramanian, Coordinate Transformation, Orthogonal Collocation, Model Reformulation and Simulation of Electrochemical-Thermal Behavior of Lithium-Ion Battery Stacks, Journal of The Electrochemical Society 158 (12) (2011) A1461. doi:10.1149/2.058112jes.
URL http://jes.ecsdl.org/cgi/doi/10.1149/2.058112jes

[10] S. J. Moura, F. B. Argomedo, R. Klein, A. Mirtabatabaei, M. Krstic, Battery State Estimation for a Single Particle Model With Electrolyte Dynamics, IEEE Transactions on Control Systems Technology 25 (2) (2017) 453–468. doi:10.1109/tcst.2016.2571663.

[11] A. M. Bizeray, J.-H. Kim, S. R. Duncan, D. A. Howey, Identifiability and parameter estimation of the single particle lithium-ion battery model, IEEE Transactions on Control Systems Technology (99) (2018) 1–16.

[12] M. Guo, G. Sikha, R. E. White, Single-particle model for a lithium-ion cell: Thermal behavior, Journal of The Electrochemical Society 158 (2) (2011) A122–A132.

[13] S. Dey, B. Ayalew, P. Pisu, Combined estimation of state-of-charge and state-of-health of li-ion battery cells using smo on electrochemical model, in: 2014 13th International Workshop on Variable Structure Systems (VSS), IEEE, 2014, pp. 1–6.

[14] P. Kemper, D. Kum, Extended single particle model of li-ion batteries towards high current applications, in: Vehicle Power and Propulsion Conference (VPPC), 2013 IEEE, IEEE, 2013, pp. 1–6.

[15] H. E. Perez, X. Hu, S. J. Moura, Optimal Charging of Batteries via a Single Particle Model with Electrolyte and Thermal Dynamics (10) (2016) 4000–4005.

[16] E. Prada, D. Di Domenico, Y. Creff, J. Bernard, V. Sauvant-Moynot, F. Huet, Simplified electrochemical and thermal model of lifepo4-graphite li-ion batteries for fast charge applications, Journal of The Electrochemical Society 159 (9) (2012) A1508–A1519.

[17] X. Han, M. Ouyang, L. Lu, J. Li, Simplification of physics-based electrochemical model for lithium ion battery on electric vehicle. part ii: Pseudo-two-dimensional model simplification and state of charge estimation, Journal of Power Sources 278 (2015) 814–825.

[18] S. K. Rahimian, S. Rayman, R. E. White, Extension of physics-based single particle model for higher charge–discharge rates, Journal of Power Sources 224 (2013) 180–194.

[19] T. R. Tanim, C. D. Rahn, C.-Y. Wang, A temperature dependent, single particle, lithium ion cell model including electrolyte diffusion, Journal of Dynamic Systems, Measurement, and Control 137 (1) (2015) 011005.

[20] E. Hinch, Perturbation methods. 1991.

[21] C. M. Bender, S. A. Orszag, Advanced mathematical methods for scientists and engineers I: Asymptotic methods and perturbation theory, Springer Science & Business Media, 2013.

[22] G. Richardson, G. Denuault, C. P. Please, Multiscale modelling and analysis of lithium-ion battery charge and discharge, Journal of Engineering Mathematics 72 (1) (2012) 41–72. doi:10.1007/s10665-011-9461-9.
URL http://link.springer.com/10.1007/s10665-011-9461-9

[23] V. Sulzer, S. J. Chapman, C. P. Please, D. A. Howey, C. W. Monroe, Faster lead-acid battery simulations from porous-electrode theory: Ii. asymptotic analysis, arXiv preprint arXiv:1902.01774 (2019).

[24] I. R. Moyles, M. G. Hennessy, T. G. Myers, B. R. Wetton, Asymptotic reduction of a porous electrode model for lithium-ion batteries, arXiv preprint arXiv:1805.07093 (2018).

[25] J. Newman, Dualfoil, http://www.cchem.berkeley.edu/jsngrp/fortran.html (2014).

[26] S. Moura, fastdfn, https://github.com/scott-moura/fastDFN (2016).

[27] A. M. Bizeray, J.-H. Kim, S. R. Duncan, D. A. Howey, Identifiability and parameter estimation of the single particle lithium-ion battery model (2017). arXiv:1702.02471.
URL http://arxiv.org/abs/1702.02471